Design of Arrays with Mutual Coupling

A Project submitted to
VISVESVARAYA TECHNOLOGICAL UNIVERSITY
Belagaum
in partial fulfilment of the requirements for the award of degree of

Bachelor of Engineering in
Electronics and Communication

by

Anuktha S Nayak
Ramyashree V Bhatt
Varsha V

Electronics and Communication Engineering
PESIT

2013/2017

Declaration

We hereby declare that the project report entitled **Design of Arrays with Mutual Coupling** is the bonafide record of the project carried out at **P.E.S. Institute of Technology** in partial fulfilment of the requirements for the award of degree of **Bachelor of Engineering** in **Electronics and Communication** of **Visvesvaraya Technological University, Belgaum** during the academic year 2016-17. We further declare that the project report is not submitted to any other universities in fulfilment of the requirements for the award of any degree.

Anuktha S Nayak (1PI13EC125)
Ramyashree V Bhat(1PI13EC076)
Varsha V(1PI13EC115)

Visvesvaraya Technological University
Belgaum - 590014

PES Institute of Technology
(An Autonomous Institute under VTU, Belgaum)
Bangalore - 560085

CERTIFICATE

This is to certify that the project entitled **Design of Arrays with Mutual Coupling** is a bonafide work carried out by **Ramyashree V Bhat**, **Varsha V** and **Anuktha S Nayak** bearing University Seat Numbers **1PI13EC076**, **1PI13EC115** and **1PI13EC125** respectively in partial fulfilment of the requirements for the award of **Bachelor of Engineering** in **Electronics and Communication** from **Visvesvaraya Technological University, Belgaum** during the academic year 2016-17. The project report has been approved as it satisfies the academic requirements prescribed for the award of the said degree.

HoD
Dr.Chandar T.S
Dept. of ECE
PESIT

Guide
Dr.Saumya Adhikari
Dept. of ECE
PESIT

Principal
Dr.K.S Sridhar
PESIT

External Viva :
Name of the Examiner with Signature and Date
1.
2.

Abstract

Directivity of an antenna is of great consequence in the area of wireless communication. In order to enhance directivity, an array is made use of. The structure of an array involves the antenna elements and the feed network. Most arrays have a corporate feed network making it complex and bulky. In this project a single pair of transmission lines is used to excite the dipoles connected in parallel. The concept of varying the lengths of the array elements so as to obtain the desired resistance is presented. This makes the need for additional resistive elements redundant and thus efficiency is enhanced due to the absence of I^2R loss. The inter-element spacing in the array is maintained at 0.25λ thereby ensuring better control over the side lobe levels. However, at this spacing mutual coupling effect is very strong and hence suitable changes are made to the array design to mitigate its effects. Further, highly directive endfire arrays have been designed using modified Chebyshev variant polynomials.

Acknowledgement

On the submission of our final year project entitled **Design of Arrays with Mutual Coupling**, we would like to express our deep gratitude to our project supervisor **Dr.Saumya Adhikari**, Associate Professor, Department of Electronics and Communication Engineering, PES Institute of Technology for his inspiration and encouragement during the course of our project work. We truly appreciate his guidance and support right from the beginning to the very end of this work.

We would like to sincerely thank **Dr.Chandar T.S** for his motivation and support during the course of this project.

We are thankful to our internal panel, whose valuable comments and suggestions assisted us in completing this project.

We extend our gratitude to Mr. C.S Shiva Shankar for providing us a suitable environment to work in. We are grateful to the non-teaching staff of the Department of Electronics and Communication for their support during the course of this project.

Last, but not the least, we wish to thank our family and friends for their support and encouragement.

Anuktha S Nayak
Ramyashree V Bhat
Varsha V

Contents

List of Figures

Chapter 1

Introduction

Wireless communication usurped much of the data sharing domain with its outbreak in the nineteenth century. Antenna being an integral part of such a system has been studied for centuries to enhance the performance of the system. Directivity of an antenna is the primary factor that determines the gain of an antenna. By definition, it is the ratio of the maximum power to the total power radiated. This gives an idea about the strength of the signal in a specific direction. A single antenna cannot produce a very directive beam because of its limited aperture. For this reason, an array is built which can be made up of uniform elements or a motley of different antennas. The directivity increases with the number of elements in an array, Fig. 1.1.

An array can be categorized as broadside or endfire depending on the location of

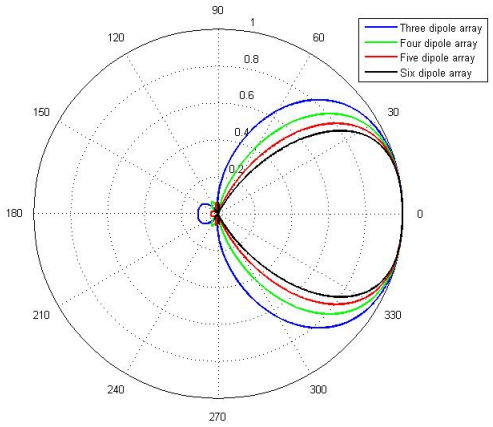

Figure 1.1: Radiation pattern of arrays of different number of elements

the main lobe. Most arrays are broadside and have a corporate feed. The feed network is complicated and bulky, Fig.1.2. In the present work, an endfire array has been designed which has better directivity than a broadside and all dipoles are connected to the same pair of transmission line with its width maintained constant. The inter-element spacing is maintained at 0.25λ. At such a low spacing, the effect of mutual coupling is very pronounced. The spacing between the individual elements of an array must be maintained at 0.25λ so as to reduce the back lobe and achieve stringent control over radiation pattern. Under the influence of mutual coupling the current in a particular element of an array depends on the excitation voltage across its terminals and also on the radiation from its neighboring antennas as shown in Fig.

1.3. In the structure presented in this project, the lengths of the dipoles are varied. This takes away the need for additional resistive elements as the radiation resistance of the dipoles alone suffice, making it compact and avoiding I^2R loss.

The effects of mutual coupling was studied in this project and different methods of

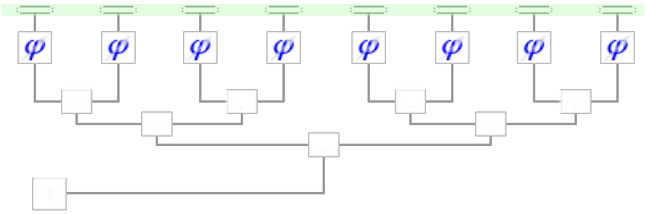

Figure 1.2: Corporate Feed Network

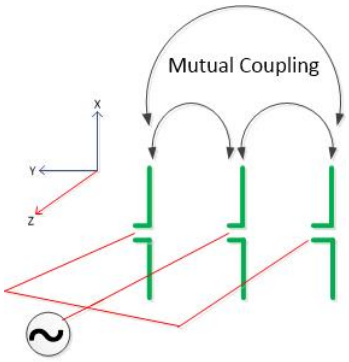

Figure 1.3: Mutual coupling interference on adjoining elements

tackling it were devised. Uniform endfire arrays were designed using this structure and codes were written. A good agreement between the results obtained using code and HFSS simulations results was observed.Material for HFSS Study, **Source** $http://e-science.ru/sites/default/files/upload\_forums\_files/8u/HFSSintro.pdf$. High directive antennas were designed and results were compared. An improvement upto 3.09dB was seen.

1.1 Outline of the Report

The report has been organized in the following manner,
Chapter 2 deals with the existing work on mutual coupling and its effects. A survey of the structures designed to improve directivity has been carried out.
The problem statement and the objectives of the project are explained in chapter 3.
Chapter 4 explains the formulation of the problem which includes a discussion on the basic parameters required to be considered along with the approach used to design and analyze the problem. This chapter also contains the different algorithms that were developed and executed. Further, the synthesis of highly directive arrays using the modified Chebyshev polynomial is discussed.
Chapter 5 compares preliminary results obtained using the code and HFSS simulations. Since HFSS simulations are a closer estimate to practical values, necessary calibrations which are required to be made have been discussed.
Chapter 6 discusses the numerous results obtained and inferences that can be drawn

from them.
Chapter 7 concludes the report. The insights generated from the research work have been highlighted in this chapter. Momentum for further improvement of the directivity using the concept of modified Chebyshev polynomial has been explained.
Relevant codes are given in the appendix.

Chapter 2

Literature Survey

Antenna Arrays are designed with Mutual Coupling effect compensation to make it more suitable for practical applications. This has been a topic of research for a long time and is still hot in pursuit. Work in [13] compensates for Mutual Coupling effect using genetic algorithm after finding voltages at all the existing ports taking mutual coupling into account. Mutual coupling compensation has also been carried out by applying voltages at the port such that the effective voltage after mutual coupling effect is the same as the desired voltage using the concept of matrix multiplication in [5]. Work in [1] compensates Mutual Coupling effects by using feed-forward technique to antennas in array, currents in the antenna are maintained such that the induced current is always out of phase with the existing current thereby reducing mutual coupling effects.

Few existing methods to compute Mutual impedance include Moment Method [3] which is an elaborative method which is time consuming and complex, and Induced EMF Method [2]. The latter ahs been used in this project. Work in [13] computes Mutual Coupling coefficients from S parameters.Work in [9] provides Mutual Coupling estimation procedure by finding relation between transfer function of antenna in transmitting mode and receiving mode.

After computing Mutual Coupling effect, this must be included in equations prior to compensation. Work in [2] considers Mutual Coupling as a Current Controlled Voltage Source for coupled antennas has been used in this project. Equations used depends on the structure of array. Various structure of arrays like series feed and corporate feed exist as in [2]. For these structure, port voltages can be computed with ease along with mutual coupling effect.

The structure used in this project has a unique way of interconnecting arrays, in which radiation resistance of one antenna provides feed to succeeding antenna. For this structure, compensation of mutual coupling is carried out by varying lengths of antennas in the array. The equivalent circuit of the dipole is arrived at in the manner described in [6] along with its mutual coupling effects at its antenna port. An analysis of half wave dipole array with low spacing between the elements and an analysis using the equivalent circuit is carried out in [10]. An uniform endfire array has been designed in this project maintaining low inter-element spacing. Work in [12] presents a plausible design for uniform endfire array.

The main reason behind mutual coupling compensation is to achieve a better radiation pattern. Further, it is required that the half power beam width of the antenna be as low as possible so as to improve the directivity. Particularly for end-fire arrays, [14] carries out an enhancement of the directivity of the array and simultaneously carries out a reduction in the side lobe level using the Chebyshev variant polynomial. Many approaches have been adopted to design super directive arrays. The theoretical and practical limitations of the construction of super directive arrays has been elucidated

in [8]. Work in [4] makes use of a polynomial method to construct superdirective arrays with high effieciency. Super directive arrays with low inter-element spacing has been constructed and ways to reduce the coupling between the elements has been explained in [7].

Chapter 3

Problem Definition

The first phase of the project involves the study of the various parameters affecting the radiation pattern of an antenna with a focus on mutual coupling. Necessary equations are derived and their values are varied for different conditions to understand their properties. In the second phase, algorithms are developed to arrive at the desired design. Codes are written using Matlab and C programming language; simulation is carried out on HFSS. The structure is first designed to cater to the requirements of uniform endfire array with mutual coupling taken into consideration. It is then developed to obtain highly directive endfire arrays using the modified Chebyshev variant polynomial.

3.1 Problem Statement

Design and Analysis of arrays of dipoles with *varying lengths* taking **Mutual Coupling** into account.

3.2 Objectives

The objectives of our project include,

1. Study the effects of mutual coupling and devise ways to tackle it when inter-element spacing is low. With low inter-element spacing, stringent control over radiation pattern can be achieved.

2. Design an uniform endfire array with low inter-element spacing.

3. Design highly directive endfire arrays using the modified Chebyshev variant polynomial.

3.3 Project constraints

On the theoretical front, assumptions regarding the materials have been made, in that they are considered ideal-perfectly conducting. The dipoles are assumed to be very thin and mutual coupling arising from transmission lines has been neglected. The interlinking transmission lines are assumed to be lossless.

3.4 Software requirements

All the codes are written on Matlab and/or C programming language. The results obtained are simulated on HFSS.

HFSS is a commercial finite element method solver for electromagnetic structures from Ansys. The acronym originally stood for high frequency structural simulator. It is one of several commercial tools used for antenna design, and the design of complex RF electronic circuit elements including filters, transmission lines, and packaging. Thousands of engineers have used HFSS in the analysis of electromagnetic components. Initially used to model waveguide transitions, HFSS was quickly utilized for other engineering design challenges. HFSS is now used by designers in all segments of the electronics industry. HFSS often is used during the design stage, and is an integral part of the design process.

There are six main steps in creating and solving a HFSS simulation,

1. Create model/ Geometry: The initial task in creating an HFSS model consists of the creation of the physical model that a user wishes to analyze. This model creation can be done within HFSS using the 3D modeller. The 3D modeller is fully parametric and will allow a user to create a structure that is variable with regard to geometric dimensions and material properties. A parametric structure, therefore, is very useful when final dimensions are not known or design is to be "tuned."

2. Assign Boundaries: The assignment of "boundaries" generally is done next. Boundaries are applied to specifically created 2D (sheet) objects or specific surfaces of 3D objects. Boundaries have a direct impact on the solutions that HFSS provides; therefore, users are encouraged to closely review the section on Boundaries in this document.

3. Assign Excitations: After the boundaries have been assigned, the excitations (or ports) should be applied. As with boundaries, the excitations have a direct impact on the quality of the results that HFSS will yield for a given model.

4. Set up the solution: Once boundaries and excitations have been created, the next step is to create a solution setup. During this step, a user will select a solution frequency, the desired convergence criteria, the maximum number of adaptive steps to perform, a frequency band over which solutions are desired, and what particular solution and frequency sweep methodology to use.

5. Solve: When the initial four steps have been completed by an HFSS user, the model is now ready to be analyzed. The time required for an analysis is highly dependent upon the model geometry, the solution frequency, and available computer resources.

6. Post – process the results: Once the solution has finished, a user can post-process the results. Post processing of results can be as simple as examining the S-parameters of the device modelled or plotting the fields in and around the structure. Users can also examine the far fields created by an antenna. In essence, any field quantity or S,Y,Z parameter can be plotted in the post-processor. Additionally, if a parameterized model has been analyzed, families of curves can be created.

Source: e-science.ru/sites/default/files/upload_forums_files/8u/HFSSintro.pdf

Chapter 4

Problem Formulation

The aim of the project is to design endfire arrays considering mutual coupling. For this purpose, the lengths of the dipoles are varied so as to provide the desired resistance. This way, there would be no requirement for additional resistive elements in the design and this would ideally make the I^2R loss zero. In order to understand what the desired length must be, the relation between the lengths of the dipole and its resistance must be known. Along with this, several other parameters affecting the radiation pattern needs to be understood. The analysis of the various parameters affecting the design constraints are explained in Section. 4.1.

4.1 Basic Design Parameters

In this secction, the parameters needed to be considered for the analysis of arrays are discussed.

4.1.1 Radiation Resistance and Input Resistance

Consider a finite length dipole with length $\leq 0.5\lambda$ shown in Fig. 4.1,

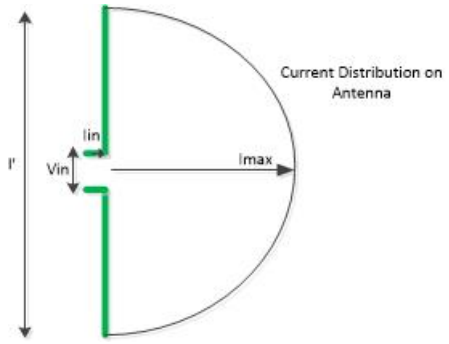

Figure 4.1: Finite element dipole

$$V_{in} = Z_{in} I_{in} \tag{4.1}$$

Here, V_{in} - Input Voltage, I_{in} - Input Current
Z_{in} - Input Impedance, l' is the length of the dipole
R_{in} - Input Resistance, X_{in} - Antenna Reactance

The current distribution on a dipole is given as,

$$I(z') = I_{max} sin(\frac{2\pi}{\lambda}(\frac{l'}{2} - |z'|)) \tag{4.2}$$

The current at the feed point where $z' = 0$ is the input current. It is given as,

$$I_{in} = p * I_{max} \tag{4.3}$$

where,

$$p = \begin{cases} 1, & \text{if } l' < \frac{\lambda}{2} \\ sin(\frac{kl'}{2}), & \text{otherwise} \end{cases} \tag{4.4}$$

Radiation Resistance(R_r) is a hypothetical resistance which indicates the amount of power radiated into free space. The resistance across the terminals of an antenna is termed as **Input Resistance** and it is equal to radiation resistance when length of dipole is $\leq 0.5\lambda$. The input resistance is also referred to as the self impedance of an antenna.
Radiation resistance is derived by equating the input power and the radiated power (assuming dipole is made of a perfect conductor).

$$P_{rad} = I_{max}^2 R_r = P_{in} \tag{4.5}$$

$$I_{max}^2 R_r = I_{in}^2 R_{in} \tag{4.6}$$

Substituting for I_{in} and simplifying, R_{in} is obtained as,

$$R_{in} = R_r / p^2 \tag{4.7}$$

In this context, the dipole has finite length so the corresponding Electric(E) and Magnetic Field(H) for finite length dipole are derived by dividing it into hertzian dipoles and using the results of the hertzian dipole to integrate over the entire length. Using E and H, P_{rad} is calculated using Poynting theorm, given by equation 4.8. Equations 4.5 and 4.8 are equated to obtain the radiation resistance as given by equation 4.9.

$$P_{rad} = \frac{1}{2}[E \times H^*].\hat{a}_p \tag{4.8}$$

$$R_r = 60 \int_0^{\pi} \frac{(cos(\frac{kl'}{2}cos(\theta)) - cos(\frac{kl'}{2}))^2}{sin(\theta)} d\theta \tag{4.9}$$

Fig. 4.2 shows the variation of radiation resistance and input resistance with the length of the dipole plotted using equation 4.9 on MATLAB.

4.1.2 Mutual Impedance

When two antennas are placed close to each other, radiation from one antenna induces a voltage in the other antenna altering the voltage across that antenna thereby changing the current distribution. Detailed analysis of mutual impedance and its derivation is given in Section. 4.2.

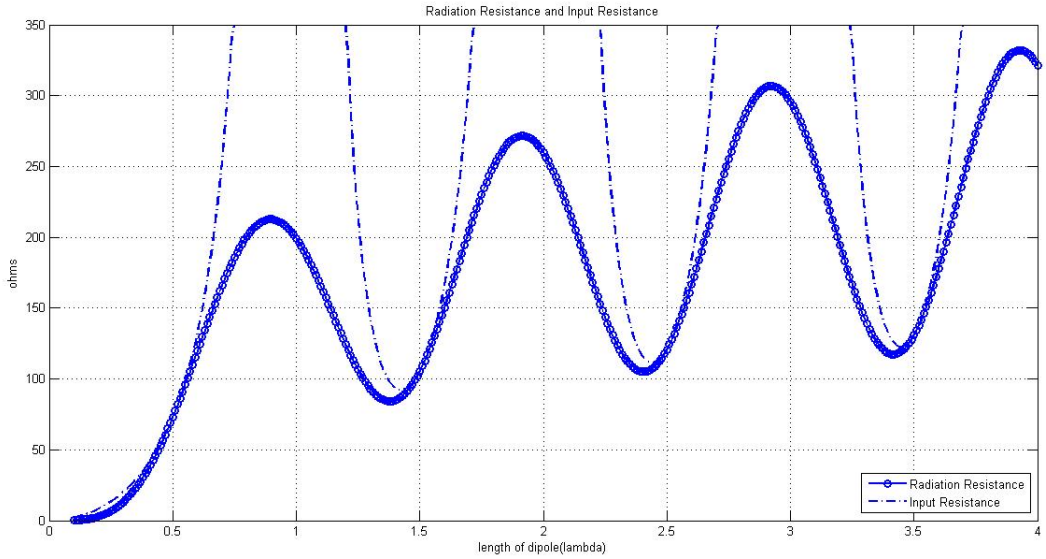

Figure 4.2: Input resistance and radiation resistance versus length of dipole

4.1.3 Antenna Reactance

Antenna impedance can be given as [2],

$$R_A = R_r + X_m \tag{4.10}$$

where R_r denotes the radiation resistance and X_m the antenna reactance. The reactance is present as the current and the voltage will not always be in phase with one another and it is used to denote the phase between the two quantities. This value can be modified by adding stubs in the dipole.

4.1.4 Characteristic Impedance of transmission line

Characteristic Impedance of transmission line is the impedance offered by the transmission line. It can be calculated as follows,

$$Z_0 = 120ln(\frac{d}{a})$$

Where d - distance between the center's of both transmission line.
a - radius of each wire in transmission line.
The value of Z_0 must be greater than 80Ω which happens when d is greater 2a. When d=2a, the two lines touch one another. But even this value will not be sufficient. To estimate the value close to practical values required for Z_0, HFSS simulations are carried out. To find the value of Z0 of a two wire transmission line in HFSS, the following steps are carried out:

- The short circuit load is taken and the input impedance at l = $\lambda/4$ is measured in HFSS.
- This ideally gives the Zin (the input impedance) value as infinity, but practical (HFSS) values are noted down.

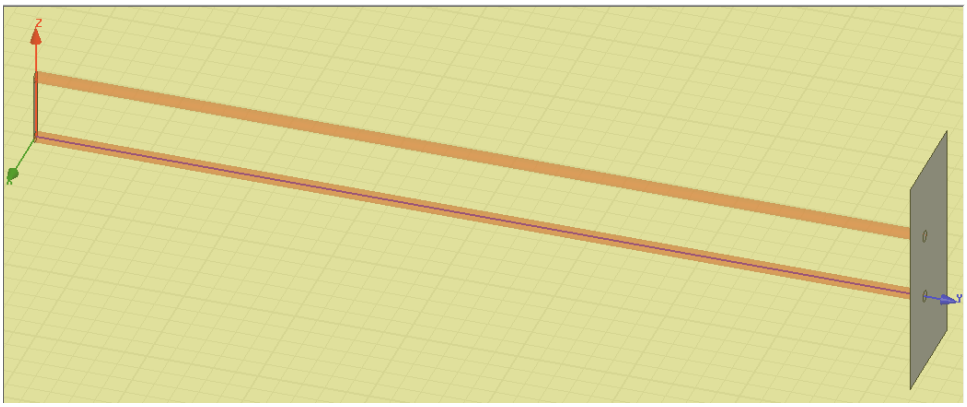

Figure 4.3: Representation of transmission line on HFSS

Table 4.1: HFSS results for Z_{in}

d/a	$Z_{in}(\Omega) = (Z_0)^2/Z_L$
4	50-7135j
6	74.53-7238.3j
8	115.38-7763.4j
10	116.01-6780.4j
12	152.67-6978.4j

- These values are noted down for different d/a values and are tabulated.
- The input impedance of the two wire transmission line is given by the formula

$$Z_{in}(l) = Z_0 \frac{Z_L + jZ_0 tan(\beta l)}{Z_0 + jZ_L tan(\beta l)} \tag{4.11}$$

  where, Z_0 is the characteristic impedance of the transmission line,
  Z_L is the impedance of the load,
  $\beta = 2\Pi/\lambda$, λ is the wavelength,
  l is the length of the transmission line.

- For $l = \lambda/4$, Zin = (Z0)2 / ZL

$$Z_{in} = (Z_0)^2/Z_L \tag{4.12}$$

- Now the 0.48λ dipole ($Z_L = (74 + 5j)\Omega$) is placed as the load.
- The Z_{in} is noted down from HFSS.
- The above step is first carried out for the various values of d/a (ranging from 4 to 12), for a particular length of the transmission line.
- Similarly, the Z_{in} is noted for various length of the transmission line (ranging from 0.1λ to 0.4λ).
- The impedance of dipole is substituted for Z_L and by combining equations 4.11 and 4.12; the value of Z_0 is calculated. The calculated Z_0 for one of the lengths is tabulated below,

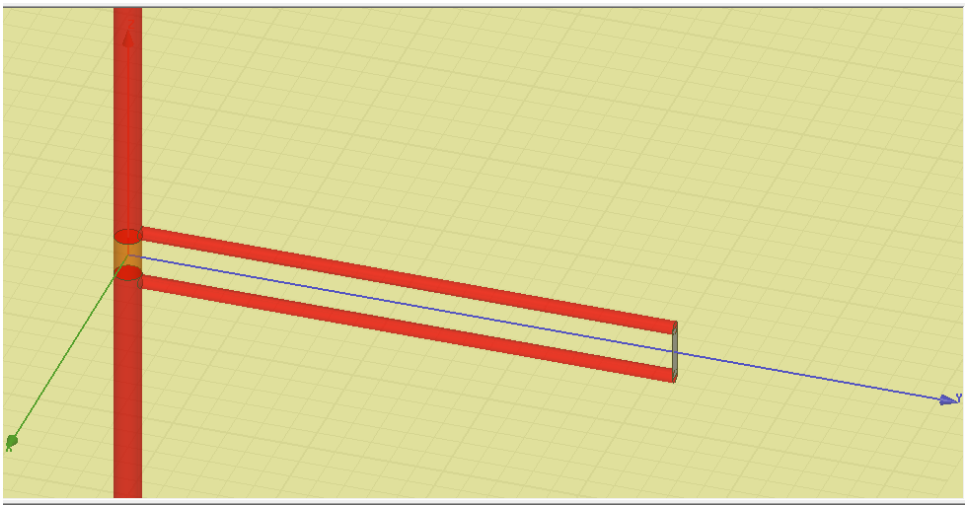

Figure 4.4: Representation of dipole and transmission line on HFSS

Table 4.2: HFSS results

d/a	$Z_{in}(\Omega)$ (l = 0.1λ)
4	0.0090389+117.87j
6	0.0088245+119.45j
8	0.024+158.93j
10	0.047+184.32j
12	0.0725+210.96j

Table 4.3: HFSS results

d/a	$Z_{in}(\Omega)$ (l = 0.2λ)	$Z_{in}(\Omega)$ (l = 0.3λ)	$Z_{in}(\Omega)$ (l = 0.4λ)
4	1.534+864.8j	1.2873-684.63j	0.043-108.33j
6	4.3827+1098.8j	2.8342-795.05j	0.1134-135.23j
8	7.5188+1243.5j	4.8059-851.59j	0.20398-165.97j
10	10.74+1378.8j	7.2805-914.24j	0.32378-181.53j
12	21.272+1625.7j	10.056-920.54j	0.4809-192.25j

Table 4.4: HFSS results

d/a	$Z_0(\Omega)$ (formula)	$Z_0(\Omega)$ (HFSS)
4	166	154.504+0.02j
6	215	204.44+0.048j
8	249	245.47+0.099j
10	276	271.22+0.1382j
12	298	295.34+0.202j

- For a particular length of the transmission line, the Z_0 obtained by HFSS, for the various d/a can be plotted and compared with the formula.
  Specifications:
  Frequency of operation = 750 MHz, Wavelength = 400mm
  Length of the dipole = 0.48λ = 188mm
  Thickness of the dipole = 1mm
  Feed gap length = 4mm
  a=0.5mm

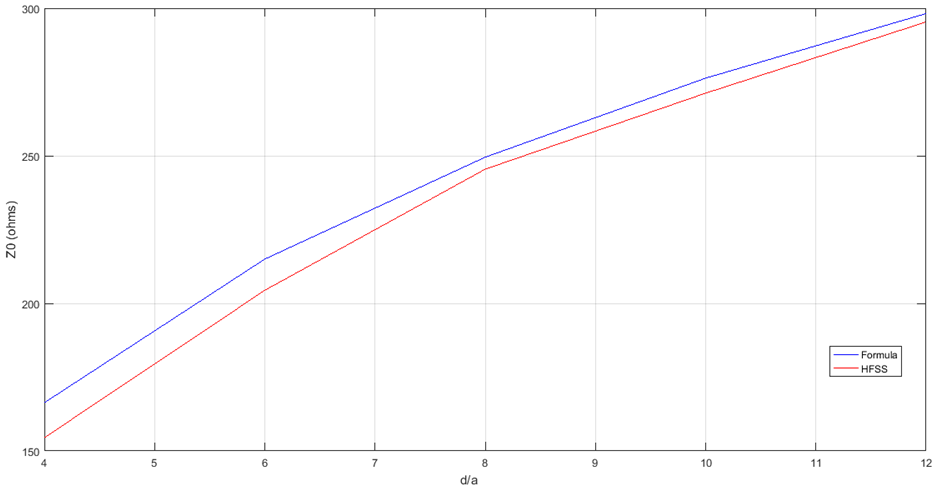

Figure 4.5: Z_0 vs transmission line length

The difference in the results is mainly because of the reason that the formula for the characteristic impedance of the transmission line does not take into account the skin effect, whereas HFSS does. Also the formula for the characteristic impedance of the transmission line is more suitable for $d >> a$, hence the difference between the theoretical and HFSS results decreases as the d/a increases.
In the formula of characteristic impedance of the transmission line, Z_0 value has to be greater than 80Ω, since $d >= 2a$. Hence the theoretical calculations are carried out for $Z_0 = 200\Omega$. From the graph ?? for $Z_0 = 200\Omega$, $d/a = 5.8$mm. On fixing a = 0.5mm, we get d = 2.9mm.
out.

4.1.5 Radiation Pattern

An array of identical elements all of identical magnitude and each with a progressive phase is referred to as a uniform array. For such arrays, there exists an array factor which is multiplied by the field pattern of an individual antenna to obtain the resultant field of the array. In the structure presented, the array elements do not have a constant length and therefore the electric field needs to be calculated for each of the elements and summed up to obtain the resultant field pattern.

4.2 Study of Mutual Coupling

When the inter-element spacing is low, the mutual coupling effect is prominent and cannot be neglected and for this reason, mutual coupling effects are included in the

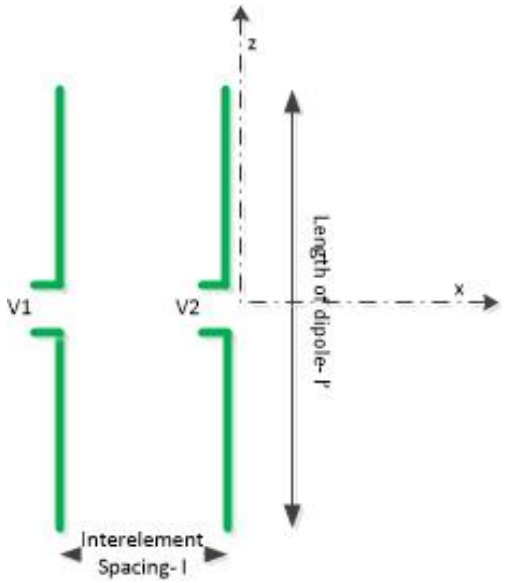

(a) Coupled Antenna Diagram (b) Equivalent Circuit Diagram of Coupled Antennas

Figure 4.6: Coupled Antennas

design of arrays.
Consider two coupled antennas placed as shown in Fig. 4.6a.

Mutual coupling effects can be depicted in an array design as current controlled voltage source. Fig.4.6b shows the equivalent circuit diagram of coupled antennas. Here, Z_{11} - Self Impedance (Input Impedance) of dipole 1.

Z_{22} - Self Impedance (Input Impedance) of dipole 2.

Z_{12}, Z_{21} - Mutual Impedance between dipoles 1 and 2.

Z_{12} denotes the mutual impedance arising due of the voltage induced on dipole 1 by dipole 2.

There exists many methods to calculate mutual impedance as explained in the literature survey. In this project, the induced emf method has been used to calculate the mutual impedance. It involves the computation of the induced voltage from which the mutual impedance is derived. The voltage induced by dipole 1 on dipole 2 is represented as V_{12} and the following relations can be drawn,

$$Z_{12} = -V_{12}/I_{2max}; \qquad Z_{21} = -V_{21}/I_{1max}; \tag{4.13}$$

The voltage induced is be found to be,

$$V_{12} = -\frac{1}{I_{1max}} \int_{-\frac{l'_2}{2}}^{\frac{l'_2}{2}} E_{Z21}(z') I_2(z') dz' \tag{4.14}$$

Combining equations 4.13 and 4.14 general equation for mutual impedance is obtained as,

$$Z_{12} = -\frac{1}{I_{1max} I_{2max}} \int_{-\frac{l'_2}{2}}^{\frac{l'_2}{2}} E_{Z21}(z') I_2(z') dz' \tag{4.15}$$

From reciprocity theorem, it can be proved that $Z_{21} = Z_{12}$. It can be observed that the mutual impedance is independent of current distribution on the dipole whereas the mutual coupling varies with the current. Equation 4.15 is the general form of

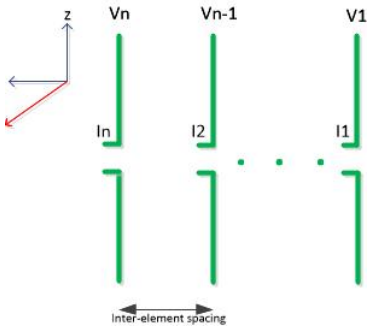

Figure 4.7: Multiple Coupled Antennas

mutual impedance for any antenna. In the next subsection, the mutual impedance specific to two dipoles is presented. In case of 'N' dipole array, Fig. 4.7, voltage at the port of each antenna will depend on the mutual coupling due to N-1 dipoles and can be written as,

$$V_1 = Z_{11}I_1 + Z_{12}I_2 + Z_{13}I_3 + ... + Z_{1n}I_n \tag{4.16}$$

.
.
.

$$V_n = Z_{n1}I_1 + Z_{n2}I_2 + Z_{n3}I_3 + ... + Z_{nn}I_n \tag{4.17}$$

4.2.1 Induced EMF Method for calculating mutual impedance

To calculate mutual impedance value from equation 4.15 the following assumptions have been made for the sake of simplicity,

1. Both dipoles are oriented long the positive z axis.
2. The maximum current (I_{max}) in both dipoles is equal to 1A.
3. Currents in the dipoles have no phase difference.

Mutual Impedance for finite length dipole is calculated by dividing into Hertzian dipoles. Hertzian Dipole is a dipole with its length($l^{'}$) very small compared to the wavelength(λ) in the range of $\lambda/20$. Let l_1 & l_2 be the lengths of dipole 1 and 2 and

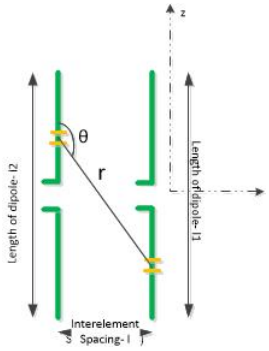

Figure 4.8: Analysis of Mutual Coupling

l be the inter-element spacing. Each dipole is split into $2N$ Hertzian dipole elements. Specifically, $2N_1$ for dipole 1 and $2N_2$ for dipole 2. N_1 & N_2 are kept such that the element lengths, $dl_1 \& dl_2$, are equal even for dipoles with unequal lengths. Let

$N_1 = 80$, then $N_2 = N_1 \frac{l_2}{l_1}$ with element lengths $dl_1 = \frac{l_1}{2N_1}$ & $dl_2 = \frac{l_2}{2N_2}$
Current Distribution on dipole 1 & 2 is given by,

$$I_1 = I_{max1} sin(\tfrac{2\pi}{\lambda}(\tfrac{l_1}{2} - |z_1|))$$

$$I_2 = I_{max2} sin(\frac{2\pi}{\lambda}(\frac{l_2}{2} - |z_2|))$$

$$I_{max1} = 1A, I_{max2} = 1A$$

z_1 for n_{th} element & z_2 for m_{th} element is given by,

$$z_1 = ndl_1, z_2 = mdl_2 \; z_1 = n\tfrac{l_1}{2N_1}, z_2 = m\tfrac{l_2}{2N_2}$$

For Hertzian Dipole with length dl and current I,

$$E_\theta = \frac{\eta I dl sin\theta}{4\pi r} e^{-\mathrm{j}kr}(\mathrm{j}k + \frac{1}{r} + \frac{1}{\mathrm{j}kr^2}) \tag{4.18}$$

$$E_r = \frac{\eta I dl cos\theta}{4\pi r} e^{-\mathrm{j}kr}(\frac{2}{r} + \frac{2}{\mathrm{j}kr^2}) \tag{4.19}$$

$\vec{E}$ on dipole 2 due to 1 arises due to the radial and the theta components of $\vec{E}$.
E_θ on the m_{th} element of dipole 2 due to dipole 1 is,

$$E_\theta = \sum_{n=-N_1}^{N_1} \frac{\eta I_1 dl_1 sin\theta}{4\pi r} e^{-\mathrm{j}kr}(\mathrm{j}k + \frac{1}{r} + \frac{1}{\mathrm{j}kr^2}) \tag{4.20}$$

$$E_\theta = \sum_{n=-N_1}^{N_1} \frac{\eta I_1 \frac{l_1}{2N_1} sin\theta}{4\pi r} e^{-\mathrm{j}kr}(\mathrm{j}k + \frac{1}{r} + \frac{1}{\mathrm{j}kr^2}) \tag{4.21}$$

Similarly for E_r,

$$E_r = \sum_{n=-N_1}^{N_1} \frac{\eta I_1 dl_1 cos\theta}{4\pi r} e^{-\mathrm{j}kr}(\frac{2}{r} + \frac{2}{\mathrm{j}kr^2}) \tag{4.22}$$

$$E_r = \sum_{n=-N_1}^{N_1} \frac{\eta I_1 \frac{l_1}{2N_1} cos\theta}{4\pi r} e^{-\mathrm{j}kr}(\frac{2}{r} + \frac{2}{\mathrm{j}kr^2}) \tag{4.23}$$

Component of E_θ and E_r in the $\vec{z}$ direction is,

$$E_z = E_\theta(-sin\theta) + E_r(cos\theta) \tag{4.24}$$

Combining equations 4.21, 4.23 and 4.24,

$$E_{z_{21}} = \sum_{n=-N_1}^{N_1} \frac{\eta I_1 \frac{l_1}{2N_1} cos\theta}{4\pi r} e^{-\mathrm{j}kr}((-sin^2\theta)(\mathrm{j}k + \frac{1}{r} + \frac{1}{\mathrm{j}kr^2}) + (cos^2\theta)(\frac{2}{r} + \frac{2}{\mathrm{j}kr^2})) \tag{4.25}$$

By Reaction Theorem,

$$V_{12} = -\frac{1}{I_{1max}} \int_{\frac{-l_2}{2}}^{\frac{l_2}{2}} (\overrightarrow{E_{z12}}.\overrightarrow{dl_2}) I_2(z) dz$$

Where $\overrightarrow{dl_2}$ is in $\vec{z}$ direction and $I_2(z')$ represents the current distribution on dipole 2. Simplifying,

$$V_{12} = \frac{1}{I_{1max}} \sum_{m=-N_2}^{N_2} \sum_{n=-N_1}^{N_1} \frac{\eta I_1 \frac{l_1}{2N_1} cos\theta}{4\pi r} e^{-\mathrm{j}kr}((-sin^2\theta)(\mathrm{j}k + \frac{1}{r} + \frac{1}{\mathrm{j}kr^2}) + (cos^2\theta)(\frac{2}{r} + \frac{2}{\mathrm{j}kr^2})) \\ dl_2 sin(\frac{2\pi}{\lambda}(\frac{l_2}{2} - |\frac{ml_2}{2N_2}|)) \tag{4.26}$$

Replacing $cos^2\theta$ by $(1 - sin^2\theta)$ & using $dl_2 = \frac{l_2}{2N_2}$ and substituting for I_1,

$$V_{12} = \sum_{m=-N_2}^{N_2} \sum_{n=-N_1}^{N_1} \frac{\eta I_{2max} \frac{l_1}{2N_1} \frac{l_2}{2N_2} cos\theta}{4\pi r} e^{-\mathrm{j}kr}((-sin^2\theta)(\mathrm{j}k + \frac{3}{r} + \frac{3}{\mathrm{j}kr^2}) + (\frac{2}{r} + \frac{2}{\mathrm{j}kr^2})) \\ sin(\frac{2\pi}{\lambda}(\frac{l_2}{2} - |\frac{ml_2}{2N_2}|))sin(\frac{2\pi}{\lambda}(\frac{l_1}{2} - |\frac{nl_1}{2N_1}|)) \tag{4.27}$$

$$V_{12} = \sum_{m=-N_2}^{N_2} \sum_{n=-N_1}^{N_1} \frac{\eta \frac{l_1}{2N_1} \frac{l_2}{2N_2} cos\theta}{4\pi r} e^{-\mathrm{j}kr}((-sin^2\theta)(\mathrm{j}k + \frac{3}{r} + \frac{3}{\mathrm{j}kr^2}) + (\frac{2}{r} + \frac{2}{\mathrm{j}kr^2})) \\ sin(\frac{2\pi}{\lambda}(\frac{l_2}{2} - |\frac{ml_2}{2N_2}|))I_{2max} sin(\frac{2\pi}{\lambda}(\frac{l_1}{2} - |\frac{nl_1}{2N_1}|)) \tag{4.28}$$

Mutual Impedance is given by $Z_{12} = \frac{V_{12}}{I_{2max}}$, where $I_{2max} = 1A$ & $Z_{12} = Z_{21}$

$$Z_{12} = \sum_{m=-N_2}^{N_2} \sum_{n=-N_1}^{N_1} \frac{\eta \frac{l_1}{2N_1} \frac{l_2}{2N_2} cos\theta}{4\pi r} e^{-\mathrm{j}kr}((-sin^2\theta)(\mathrm{j}k + \frac{3}{r} + \frac{3}{\mathrm{j}kr^2}) + (\frac{2}{r} + \frac{2}{\mathrm{j}kr^2})) \\ sin(\frac{2\pi}{\lambda}(\frac{l_2}{2} - |\frac{ml_2}{2N_2}|))sin(\frac{2\pi}{\lambda}(\frac{l_1}{2} - |\frac{nl_1}{2N_1}|)) \tag{4.29}$$

The variation of the real and imaginary parts of mutual impedance can be observed in Fig. 4.9 plotted using equation 4.29 considering half wave dipoles. The absolute value of mutual impedance is plotted in Fig. 4.10. It can be observed that the effect of mutual coupling would need to be considered at least upto 4λ.

While deriving the mutual impedance, the thickness of the dipole was considered to be almost negligible. But the practical front it is not possible to conceive such a dipole. To compare the mutual impedance values of the dipole for varying distances between them, with the theoretical values, the simulations were carried out on HFSS.

Specifications:

Frequency of operation = 750 MHz, Wavelength = 400mm

Length of the dipole = 0.48λ = 188mm

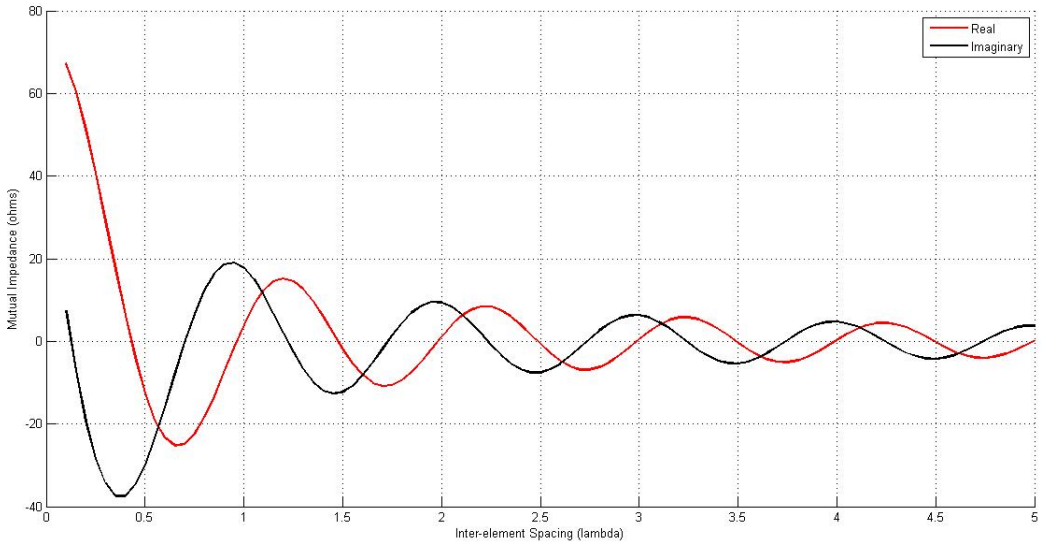

Figure 4.9: Real and Imaginary parts of Mutual Impedance vs inter-element spacing between coupled antennas

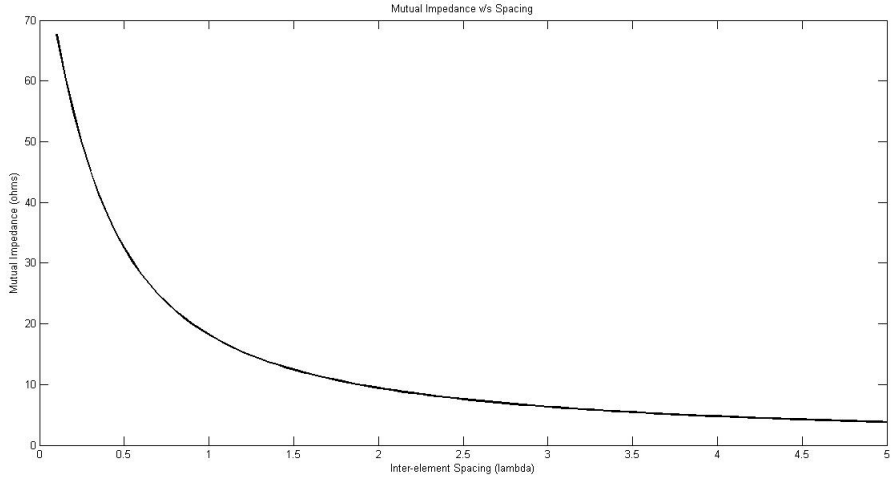

Figure 4.10: Mutual Impedance versus Inter-element spacing

Table 4.5: mutual impedance table

Distance b/n the dipole antennas(λ)	$MutualImpedance(\Omega)$
0.3	23.0780 -39.7240i
0.25	35.7730 -35.7950i
0.2	47.9470 -28.3710i
0.15	59.2560 -18.2360i
0.1	69.0570 - 5.5443i

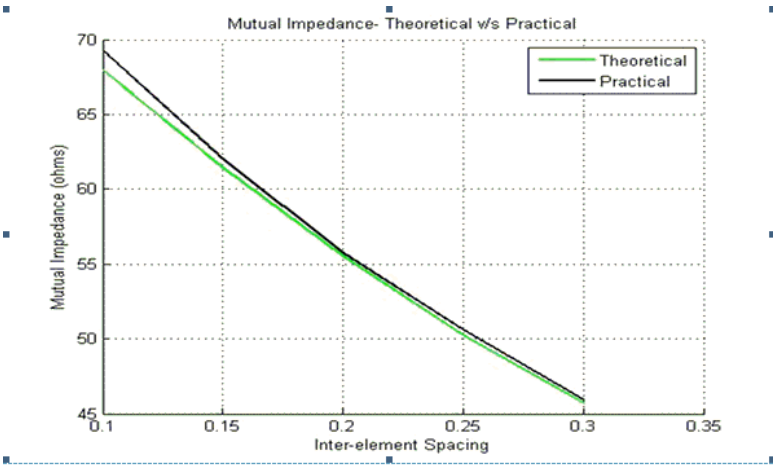

Figure 4.11: Comparison of the variation of mutual impedance versus distance for MATLAB and HFSS

Thickness of the dipole = 1mm
Feed gap length = 4mm
From the graph 4.11, we can conclude both theoretically and practically (HFSS) that the mutual impedance between the two dipoles increases with the decrease in the length between the dipoles. We can also see that, for 0.25λ the theoretical and HFSS values of mutual impedance remains almost the same. Section. 4.3 presents the structure of the array along with its analysis.

4.3 Structure of the Array- Design and Analysis

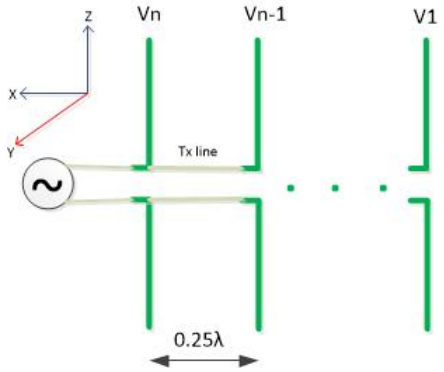

Figure 4.12: Dipole array structure

Several approaches have been adopted to combat mutual coupling as explained in the Literature Survey. In this project, the aim is to simplify the design and the structural requirements and at the same time arrive at the favored radiation pattern. Fig. 4.12 shows the arrangement of the array of finite element dipoles along the x-axis with the dipole oriented in the z-axis, fed by the generator through transmission lines. For the sake of analysis, the first pair of transmission lines are considered to be of negligible length, subsequent dipoles are parallely fed through transmission lines. This structure needs a single feed generator and requires no additional impedances, greatly simplifying the feed network and in the ideal case removes the I^2R loss completely. The radiation resistance of the dipoles are itself used to obtained the desired current

in the dipoles and this is done by *varying* the lengths of the dipoles keeping the inter-element spacing fixed at quarter of a wavelength.

4.3.1 Transmission line analysis

Transmission line analysis can be carried out either by the solution of Maxwell's field equations or by the methods of distributed-circuit theory, [11]. The solution of Maxwell's equations involves three space variables in addition to the time variable. The distributed-circuit method, however, involves only one space variable in addition to the time variable. Throughout our analysis, the latter method is used to analyze a transmission line in terms of the voltage, current, impedance, and power along the line. Based on uniformly distributed-circuit theory, the schematic circuit of a conventional two-conductor transmission line with constant parameters R, L, G, and C is shown in Fig. 4.13. The parameters are expressed in their respective names per unit length.

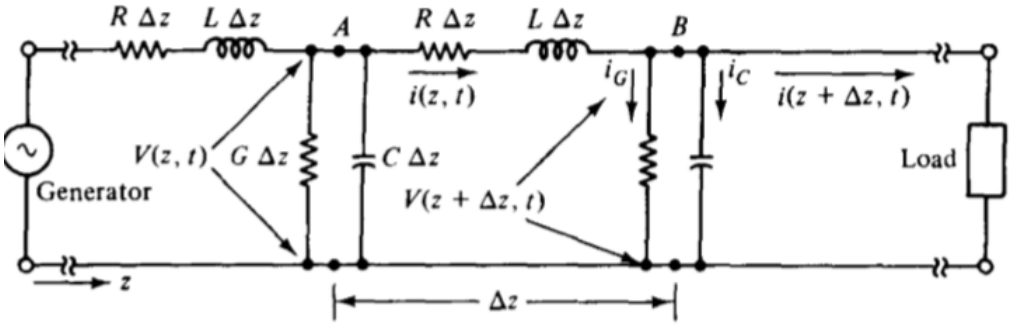

Figure 4.13: Elementary section of a transmission line, [11]

Considering this equivalent circuit, the voltage and currents at the terminal of the transmission line are determined using Kirchoff's laws. For the central loop in Fig. 4.13 of length Δz, applying KVL, we arrive at,

$$v(z,t) = i(z,t)R\Delta z + L\Delta z\frac{\partial i(z,t)}{\partial t} + v(z+\Delta z,t)$$

Dividing this by the elemental length Δz, we obtain the differential-

$$-\frac{\partial v}{\partial z} = Ri + L\frac{\partial i}{\partial t} \tag{4.30}$$

In a similar manner, KCL is used at point B and the equation obtained thus is divided by Δz to arrive at-

$$-\frac{\partial v}{\partial z} = Ri + L\frac{\partial i}{\partial t} \tag{4.31}$$

Convert equations 4.30 and 4.31 into voltage and current differential equations by differentiation and substitution of necessary terms to obtain the equations **??** and **??**.

$$\frac{\partial^2 v}{\partial z^2} = RGv + (RC + LG)\frac{\partial v}{\partial t} + LC\frac{\partial^2 v}{\partial t^2}$$
$$\frac{\partial^2 i}{\partial z^2} = RGi + (RC + LG)\frac{\partial i}{\partial t} + LC\frac{\partial^2 i}{\partial t^2}$$

The differential equations have the solution of the form $F(z)e^{j\omega t}$ with ω as a constant. Thus, the instantaneous voltage and current in a transmission line can be represented as-

$$v(z,t) = Real[V(z)e^{j\omega t}]$$
$$i(z,t) = Real[I(z)e^{j\omega t}]$$

Quantities V(z) and I(z) are complex quantities and are given as,

$$V(z) = V_+e^{-\gamma z} + V_-e^{\gamma z} \tag{4.32}$$

$$I(z) = I_+e^{-\gamma z} + I_-e^{\gamma z} \tag{4.33}$$

with γ, the propagation constant, given as,

$$\gamma = \alpha + j\beta \tag{4.34}$$

α being the attenuation constant and β the phase constant. The term involving $e^{-j\gamma z}$ represents a wave traveling in the positive z direction, and the term with the factor $e^{j\gamma z}$ is a wave going in the negative z direction. I(z) and V(z) are related as-

$$I(z) = \frac{V_+e^{-\gamma z} - V_-e^{\gamma z}}{Z_0} \tag{4.35}$$

with Z_0 as the characteristic impedance of the transmission line. The relation between the voltage and current between two points in a transmission line can be derived using equations 4.32 through 4.35. Consider Fig. 4.14 with voltage V_1 at the left extreme and voltage V_2 in the transmission line at a distance L. The complex phasor $V(z)$, equation 4.32, morphs into V_1 upon substituting z as 0 and V_2 with z as L. Similarly, equation 4.35 is used to obtain current I_1.

$$V_1 = V_+ + V_- \tag{4.36}$$

$$I_1 = \frac{V_+ - V_-}{Z_0} \tag{4.37}$$

Equations 4.36 and 4.37 are solved to get constants V_+ and V_-.

$$V_+ = \frac{V_1 + I_1Z_0}{2} \tag{4.38}$$

$$V_- = \frac{V_1 - I_1Z_0}{2} \tag{4.39}$$

Voltage and current at the right extreme of Fig. 4.14 are obtained by substituting

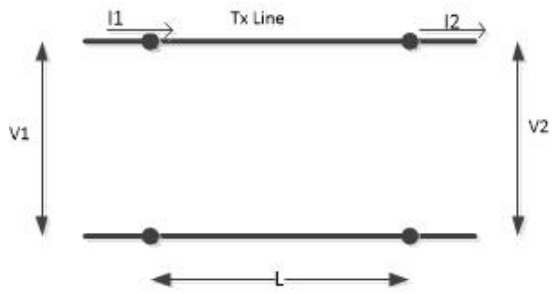

Figure 4.14: Transmission Line

z as L in equations 4.32 and 4.33 respectively. Constants V_+ and V_- are substituted

from equations 4.38 and 4.39 respectively. For simplicity of analysis, α is assumed to be zero. Thus the relationship between the electrical quantities of the transmission line are obtained.

$$V_2 = V_1 cos(\beta L) - jI_1 Z_0 sin(\beta L) \tag{4.40}$$

$$I_2 = I_1 cos(\beta L) - j\frac{V_1}{Z_0} sin(\beta L) \tag{4.41}$$

Inversely, the equations can be written as,

$$V_1 = V_2 cos(\beta L) + jI_2 Z_0 sin(\beta L) \tag{4.42}$$

$$I_1 = I_2 cos(\beta L) + j\frac{V_2}{Z_0} sin(\beta L) \tag{4.43}$$

4.3.2 Equivalent Circuit of Dipole Array

Dipole array analysis is performed by redrawing the structure as a connection of network elements as shown in Fig. 4.15 for two dipoles. Branches 1 and 2 represent the two dipoles. Each dipole can be characterized by a combination of self impedance-Z_{22}-representing the radiation resistance and reactance, and current controlled voltage sources for the mutual impedances. The self impedance is the input resistance offered by the port. The generator impedance Z_g is set such that maximum power is transferred to the dipoles for radiation. This happens when the input impedance at the generator terminal equals the conjugate of Z_g. For the sake of simplicity, this impedance is neglected at the theoretical formulation stage, but is accounted for during HFSS simulation. As explained earlier, the voltage is fed directly to the first

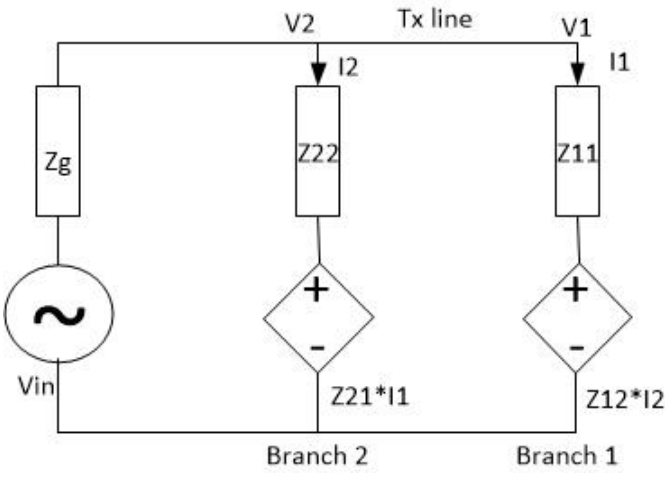

Figure 4.15: Equivalent circuit of two dipole array

dipole without the use of transmission lines. The spacing between dipoles is maintained as l whose value is $\frac{\lambda}{4}$. With these initial set of assumptions, the mathematical formulation of the problem is performed. For the two dipole equivalent circuit, the relation between voltages and currents across the two branches is given by equations 4.40 and 4.41.

4.3.3 Determination of branch Currents

The currents exciting the dipoles eventually determine the radiation pattern of the array. Deciding the branch currents is thus a pivotal part of the process that is carried out by comparing the radiation pattern which is obtained through the structure shown in Fig. 4.12 and that of the desired radiation pattern which in this case is an uniform end-fire array pattern. This section elaborates on the method which helps determine the input currents in the branches of the transmission line.

Our design considers the array along the x-axis and hence, Ψ takes the form, $kdcos\phi sin\theta + \beta$. The radiation pattern is observed on the x-y plane for reasons which will be explained subsequently. θ is therefore $\frac{\pi}{2}^c$. d is the distance between adjacent elements which from Fig. 4.15 is l and equals $\frac{\lambda}{4}$. Making these substitutions, we obtain Ψ as $\frac{\pi}{2}cos\phi + \beta$. In the case of uniform end-fire arrays, the radiation pattern must have a maximum at $\Psi = 0$. This implies β must be $\frac{-\pi}{2}$. Equation 4.44 gives the total electric field of the array.

$$E_{total} = \Sigma_n e^{j\Psi n} = \Sigma_n C_n e^{\frac{jn\pi}{2}cos\phi} \tag{4.44}$$

with the progressive phase shift, β, dictating the values of the excitation coefficients-C's.

The electric field of a dipole oriented along the z-axis is given as,

$$E_\theta(\theta,\phi) = j60\Sigma_n \frac{I_{max}^{(n)}(cos(\frac{kl_n cos\theta}{2}) - cos(\frac{kl_n}{2}))}{sin\theta} e^{\frac{j\pi n}{2}cos\phi sin\theta}$$

where $I_{max}^{(n)}$ represents the maximum current in the n^{th} element.
An uniform array by definition comprises of isotropic elements. The electric field of a finite element dipole can be simplified by fixing the value of either of the parameters-θ or ϕ. If ϕ is made 0, which means that the radiation pattern is observed along the X-Z plane, the equation reduces to,

$$E_\theta(\theta,\phi=0) = j60\Sigma_n \frac{I_{max}^{(n)}(cos(\frac{kl_n cos\theta}{2}) - cos(\frac{kl_n}{2}))}{sin\theta} e^{\frac{j\pi n}{2}sin\theta}$$

The dipole factor, $j60\frac{I_{max}^{(n)}(cos(\frac{kl_n cos\theta}{2}) - cos(\frac{kl_n}{2}))}{sin\theta}$ depends on the value of θ and hence not constant. Alternately, by fixing θ as $\frac{\pi}{2}$, the electric field transforms to,

$$E_\theta(\theta=\frac{\pi}{2},\phi) = j60\Sigma_n I_{max}^{(n)}(1 - cos(\frac{kl_n}{2}))e^{\frac{j\pi n}{2}cos\phi} \tag{4.45}$$

In this case, the dipole factor is entirely independent of the angles and thus is the closest approximate to an uniform array which requires isotropic antennas. For this reason, throughout the project θ is fixed at $\frac{\pi}{2}$ and radiation pattern is found by varying ϕ.

The net electric field of the array of dipole elements oriented along z-axis is given as,

$$E_\theta(\theta=\frac{\pi}{2},\phi) = j60\Sigma_n I_{max}^{(n)}(1 - cos(\frac{kl_n}{2}))e^{\frac{j\pi n}{2}cos\phi} \tag{4.46}$$

Upon comparing equations 4.44 and 4.46, the desired values for the currents $I_{max}^{(n)}$ are obtained.

$$I_{max}^{(n)} = \frac{C_n}{(1 - cos(\frac{kl_n}{2}))} \tag{4.47}$$

The relation between the input currents flowing into the dipoles, which are otherwise referred to as the branch currents in the equivalent circuit, and the maximum currents is,

$$I_{in}^{(n)} = p * I_{max}^{(n)} \tag{4.48}$$

where,

$$p = \begin{cases} 1, & \text{if } l_x < \frac{\lambda}{2} \\ sin(\frac{kl_x}{2}), & \text{otherwise} \end{cases} \tag{4.49}$$

Or,

$$I_{in}^{(n)} = p\frac{C_n}{(1 - cos(\frac{kl_n}{2}))} \tag{4.50}$$

from equations 4.47 and 4.48.

Equation 4.50 clearly shows the dependence of I_{in} on the length of the dipoles. This fact is made use of to establish the desired currents in the circuit. Different methods that were used to obtain the desired set of values for the lengths and impedances of the dipoles are explained in the following section.

4.4 Methods to derive the lengths of the dipole

The structure of the dipole array presented in this project requires the lengths of the individual antennas of the array to be set so as to mitigate the mutual coupling effects. The main criteria is to match the obtained and desired normalized radiation patterns, therefore *one* of the possible solution is being searched for and not the optimum solution. The following four approaches were devised for this purpose,

1. Iterative Method (I)
2. Varying Z_0 Method
3. Fixed Z_0 Method
4. Iterative Method (II)

Not all the methods worked but they were essential to formulate the final method that has been used throughout the project. In this section, an array of three dipoles has been considered. Uniform end-fire excitation coefficients-C- are used. The equivalent circuit of the array is shown in Fig. 4.16. For the equivalent circuit, the branch

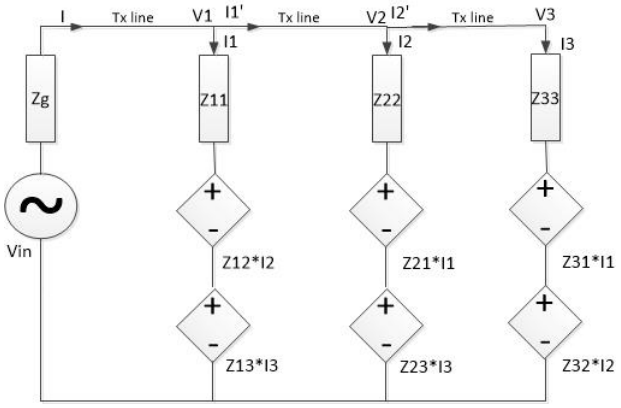

Figure 4.16: Three Dipole Equivalent Circuit

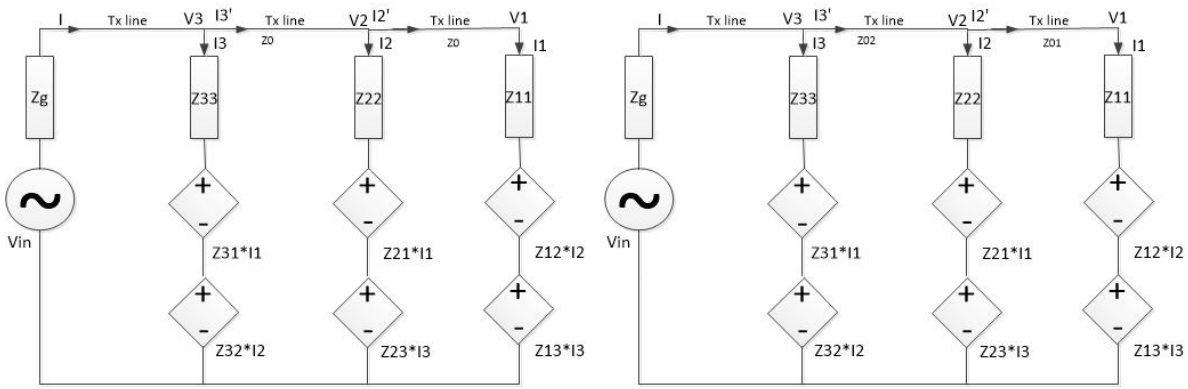

(a) Three Dipole Equivalent Circuit - Same Z0

(b) Three Dipole Equivalent Circuit - Varying Z0

Figure 4.17: Three Dipole Structure Equivalent Circuit

equations are given as,

$$V_1 = Z_{11}I_1 + Z_{12}I_2 + Z_{13}I_3 \tag{4.51}$$

$$V_2 = Z_{21}I_1 + Z_{22}I_2 + Z_{23}I_3 \tag{4.52}$$

$$V_3 = Z_{31}I_1 + Z_{32}I_2 + Z_{33}I_3 \tag{4.53}$$

List of transmission line equations, considering all transmission lines with the **same characteristic impedance** in the structure is given as,

$$V_2 = \mathrm{j}Z_0 I_1 \tag{4.54}$$

$$V_3 = \mathrm{j}Z_0 I_2 - V_1 \tag{4.55}$$

List of transmission line equations with interlinking transmission lines having **varying characteristic impedance** is given as,

$$V_2 = \mathrm{j}Z_{01} I_1 \tag{4.56}$$

$$V_3 = \mathrm{j}Z_{02} I_2 - V_1 \frac{Z_{02}}{Z_{01}} \tag{4.57}$$

4.4.1 Iterative Method (I)

Any form of iterative Method has less complexity than a brute force method. Lengths and Reactances of individual antenna elements are unknowns. Initial guess for all the lengths of dipole is considered to be 0.5λ. The number of equations is equal to the number of dipoles. The set of equations used for this method are as follows,

$$V_3 = Z_{31}I_1 + Z_{32}I_2 + Z_{33}I_3 \tag{4.58}$$

$$0 = (Z_{21} - \mathrm{j}Z_0)I_1 + Z_{22}I_2 + Z_{23}I_3 \tag{4.59}$$

$$0 = (Z_{31} + Z_{11})I_1 + (Z_{32} + Z_{12} - \mathrm{j}Z_0)I_2 + (Z_{33} + Z_{13})I_3 \tag{4.60}$$

In this method, V_3 being the input voltage supplied by the generator, its value needs to be fed. The flow chart of the steps followed in this method are mentioned in Fig. 4.18.

4.4.1.1 Drawbacks

The solution depends on the supply voltage V_3. But as the impedances and lengths have constraints on them and cannot take any value, V_3 needs to be fed prudently. Unless appropriate values for V_3 are fed, this method fails.

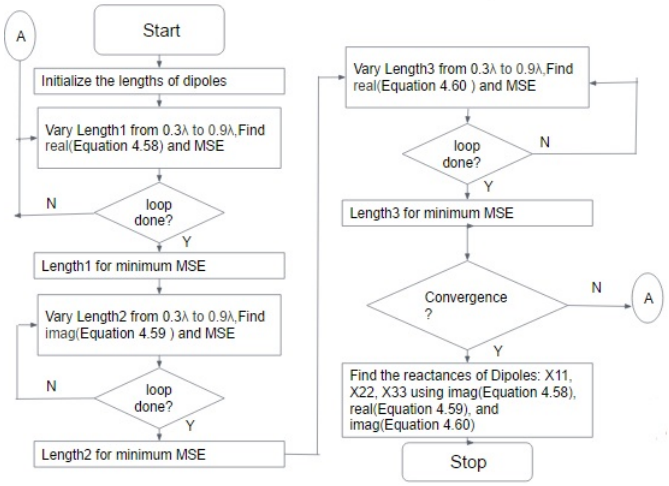

Figure 4.18: Flow Chart of Method 1

4.4.2 Varying Z_0 Method

In this method the structure was designed using transmission lines with different characteristic impedances whose values were selected so as to satisfy both the transmission line equations and the branch equations. Source voltage must be eliminated from the equations to make the solution independent of input voltage.

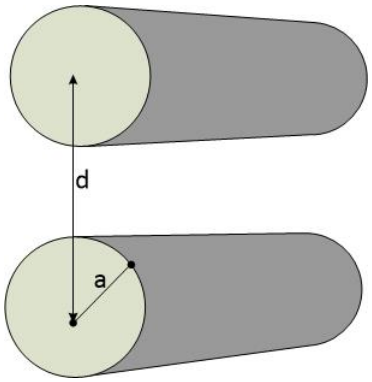

Figure 4.19: Transmission Line

4.4.2.1 Complex Z0

The set of equations used are as follows (rearranging equations 4.56 and 4.57):

$$Z_{01} = \frac{V_2}{\mathrm{j}I_1} \tag{4.61}$$

$$Z_{02} = \frac{V_3}{(\mathrm{j}I_2 - \frac{V_1}{Z_{01}})} \tag{4.62}$$

Steps followed in the method are as follows:

1. The lengths of the three dipoles are varied from 0.3λ to 0.9λ under three loops one for each of the length. The voltages V_1, V_2 and V_3 are calculated by using the branch equations. The characteristic impedance for the transmission lines are calculated using equations 4.61 and 4.62.

2. Z_{01} & Z_{02} values with $real(Z_{01})$ & $real(Z_{02}) < 80$, as Z_0 needs to be greater than 80Ω, are discarded and the iteration continues until all the values are above 80Ω.

4.4.2.2 Drawbacks

Drawbacks of the method are as follows:

1. This method gives values for Z_0 that are complex. This makes the transmission line lossy.

2. In case Z_0 is retained as a real value and a stub with the appropriate reactance is added, the complexity of the design increases and it might increase mutual coupling between the dipole and transmission line.

3. Though the lower limit on Z_0 was set at 80Ω, the actual value required was explained to be 200Ω. This constraint makes it a lot harder to arrive at a feasible solution.

4.4.2.3 Real Z0

In this method the characteristic impedance of the transmission line is retained as a real quantity.

$$Z_{01} = real(\frac{V_2}{\mathrm{j}I_1}) \tag{4.63}$$

$$Z_{02} = real(V_3/[\mathrm{j}I_2 - \frac{V_1}{Z_{01}}]) \tag{4.64}$$

$$\tag{4.65}$$

Voltage V_2 is given as,

$$V_2 = Z_{21}I_1 + Z_{22}I_2 + Z_{23}I_3$$

The self-impedance Z_{22} is modified by the addition of a reactance X_{22} introduced in the form of a stub, see Fig. 4.20. Z_{22} would then become,

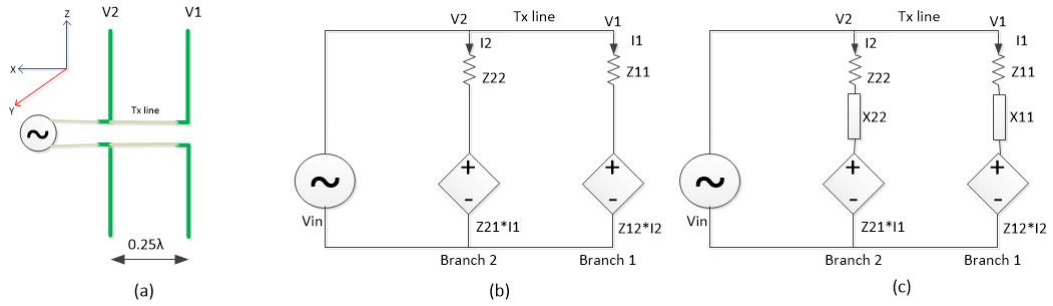

Figure 4.20: (a) Array structure, (b) Equivalent circuit, (c) Equivalent circuit with stub added for reactance

$$Z_{22} = \frac{Rr_2}{p^2} + X_{22} \tag{4.66}$$

This additional reactance is then used to compensate for the imaginary part of the RHS of equation 4.61. For the three dipole array, the equations 4.51 to 4.51, 4.56 and 4.57 are required to be satisfied. The voltages in the transmission line equations are substituted with the branch equations such that an equation with only the impedances and currents are obtained as shown,

$$Z_{21}I_1 + Z_{22}I_2 + Z_{23}I_3 - jZ_{01}I_1 = 0 = Factor_1 \tag{4.67}$$

$$Z_{31}I_1 + Z_{32}I_2 + Z_{33}I_3 + \frac{Z_{02}}{Z_{01}}(Z_{11}I_1 + Z_{12}I_2 + Z_{13}I_3) - jZ_{02}I_2 = 0 = Factor_2 \tag{4.68}$$

These equations are labeled as Factors. Now the aim is to reduce these factors to 0. In this method, the lengths of the dipoles are varied within the three loops such that this condition is met. For the case of uniform endfire, the reactances are calculated as,

$$X_{22} = imag([\mathrm{j}Z_{01}I_1 - V_2]/I_2) \tag{4.69}$$

$$X_{33} = imag([\mathrm{j}Z_{02}I_2 - V_1\frac{Z_{02}}{Z_{01}} - V_3]/I_3) \tag{4.70}$$

The reactance for dipole 1 is taken as 0. With the addition of these reactances the lengths are varied until the Factorss become zero or as close to it as possible.

4.4.2.4 Drawbacks

Drawbacks of the method are as follows:

1. With varying Z_0 values, the feed-in point has different width for every dipole.
2. This method has exponential complexity as the number of dipoles increase.

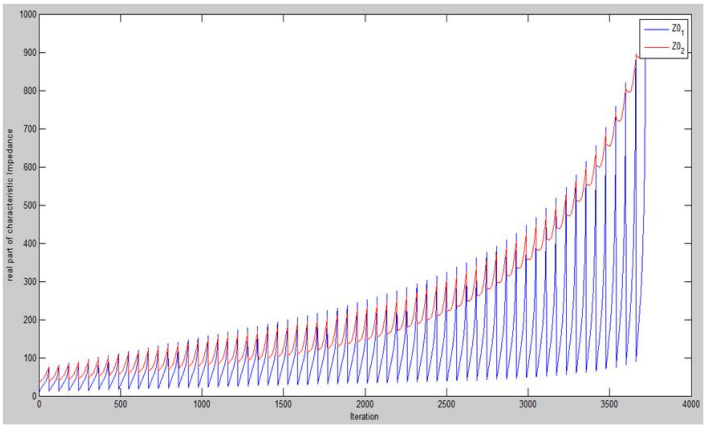

Figure 4.21: Transmission Line

4.4.2.5 Observations

An interesting result was obtained in this method by fixing the length of dipole farthest from the generator as 0.8λ for the three dipole array. $Z_{01}\&Z_{02}$ was calculated for different iterations of lengths and they were plotted on MATLAB, refer Fig. 4.21. Curves for $Z_{01}\&Z_{02}$ have overlapping points, which suggests that the transmission lines in the structure can have same Characteristic Impedance value. This led to the formulation of the next method.

4.4.3 Fixed Z_0 Method

The designed structure is less lossy and simpler if Z_0 is fixed. Unknowns are lengths and reactances of individual dipole. The set of equations used are as follows for the uniform excitation coefficients. (equations 4.51-4.55)Taking all terms to the same side:

$$(Z_{21} - \mathrm{j}Z_0)I_1 + Z_{22}I_2 + Z_{23}I_3 = 0 = Factor_1 \tag{4.71}$$

$$(Z_{31} + Z_{11})I_1 + (Z_{32} + Z_{12} - \mathrm{j}Z_0)I_2 + (Z_{33} + Z_{13})I_3 = 0 = Factor_2 \tag{4.72}$$

Specific to 3-Dipole structure, there are 6 unknowns but we have 2 complex equations, effectively 4 equations (separating real and imaginary parts). To make calculations easier $X_{11} = 0$. The steps followed in this method are:

1. Factor1 and Factor2 are calculated for all set of lengths(Note X are taken as unknowns, except $X_{11} = 0$).
2. Compensating X are found for each set of length.
3. The set (Factor1, Factor2) which gives least Mean Squared Error from (0,0) is choosen as a possible solution.

4.4.3.1 Flow Chart

Flow chart for the method is as shown in 4.22.

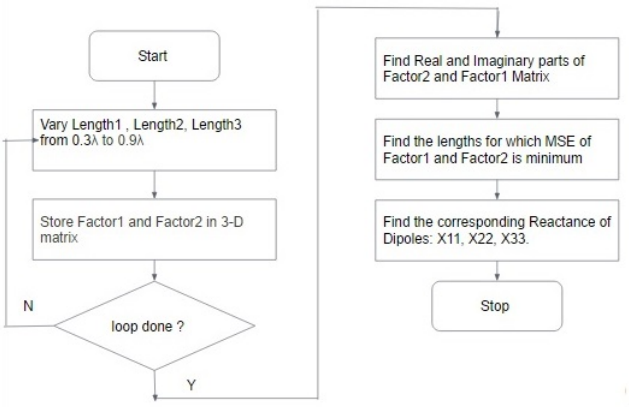

Figure 4.22: Flow Chart of Method 3

4.4.3.2 Drawbacks

Drawbacks of the method are as follows:
This is a brute force method which has been followed to verify if the designed structure has solution for fixed Z_0 value. So it has exponential complexity. This method cannot be used as the number of dipoles increase in the structure.

4.4.4 Iterative Method(II)

4.4.4.1 Description

This method has least complexity. Unknowns are lengths, reactances of individual dipole. Method 1 is being modified in this method. The set of equations used are

from equations 4.71 and 4.72. X_{11} is set as zero for convenience, convergence criteria and equations considered are as same as in Method 3.Initial guess for all the lengths of dipole is considered to be 0.5λ.

4.4.4.2 Flow Chart

Flow chart for the method is as show in Fig. 4.23.

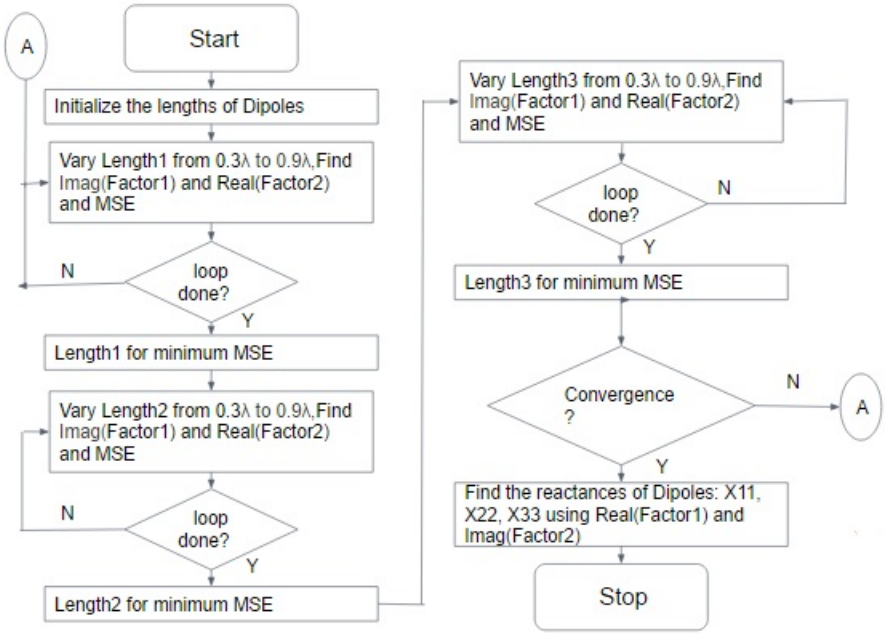

Figure 4.23: Flow Chart of Method 4

4.4.4.3 Results

The solution obtained for three dipole structure from this method are, $l_1 = 0.56300\lambda$, $l_2 = 0.84400\lambda$. $l_3 = 0.72600\lambda$, $X_{11} = 0\text{j}$, $X_{22} = 447.88\text{j}$, $X_{33} = 28.5507\text{j}$. This method has been tried for other set of initial conditions for lengths of antenna. It gives different set of converged length values.

As the results obtained using the iterative method(II) were favourable and led to a close match in the expected and obtained patterns, this method has been made use of. In the next section, a generalized set of equations to aid in the coding process has been derived for N dipoles.

4.5 Generalization

There are N branches, so N branch equations,

$$V_m = \sum_{n=1}^{N} Z_{m,n} I_n, \qquad \forall m = 1, 2, ..N \tag{4.73}$$

$$Z_{m,n} = \begin{cases} SelfImpedance(R_{m,m} + \text{j}X_{m,m}), & \text{if } m = n \\ MutualImpedance, & \text{if } m \neq n \end{cases}$$

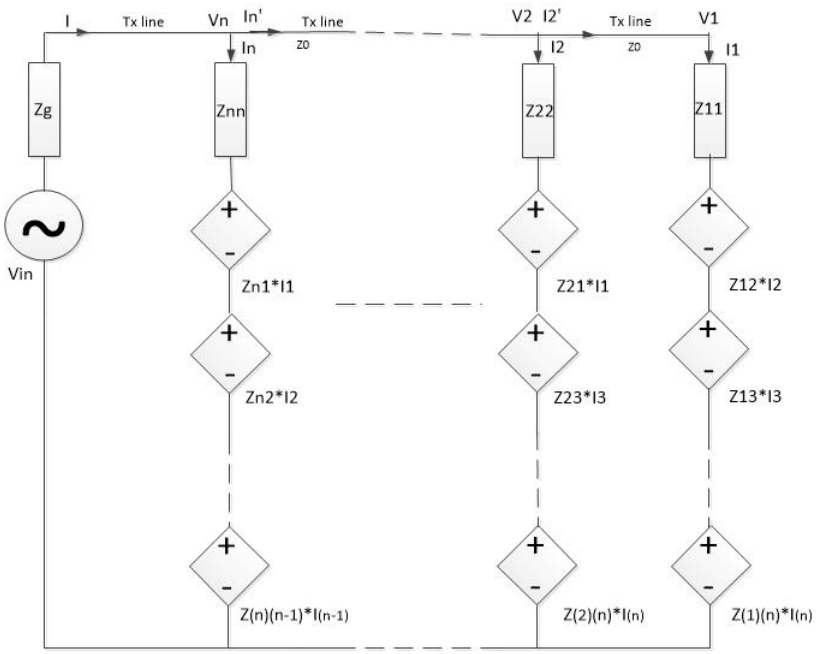

Figure 4.24: Equivalent Circuit for N dipole structure

$$I_n - current\ in\ n_{th}\ branch$$

$$R_{m,m} - Input\ Resistance,\ X_{m,m} - Reactance\ in\ m_{th}\ dipole$$

Where, $X_{m,m}$ are unknown so they are treated as 0 initially and found out after performing Iterative Method(II).

$$I_n = C_n \frac{(1 - cos\frac{kl_n}{2})}{p_n^2} \tag{4.74}$$

$I_n - current\ in\ n_{th}\ branch,\ C_n -\ Excitation\ coefficients,\ l_n - length\ of\ n_{th}\ dipole.$

$$p_n = \begin{cases} 1, & \text{if } l_n < 0.5\lambda \\ sin\frac{kl_n}{2}, & \text{if } l_n > 0.5\lambda \end{cases}$$

There are $N-1$ transmission lines in the structure where $Z_0 = 200$,

$$V_k = \begin{cases} \mathrm{j}Z_0 I_{k-1}, & \text{if } k = 2 \\ \mathrm{j}Z_0 I_{k-1} - V_{k-2}, & \text{if } k > 2 \qquad \forall k = 2,..N \end{cases} \tag{4.75}$$

Using equation 4.73 in 4.75, taking all terms to one side,

$$Factor_{(k-1)} = \begin{cases} \sum_{n=1}^{N} Z_{2,n} I_n - \mathrm{j}Z_0 i_{k-1} = 0, & \text{if } k = 2 \\ \sum_{n=1}^{N} Z_{k,n} I_n + \sum_{n=1}^{N} Z_{(k-2),n} I_n - \mathrm{j}Z_0 I_{k-1} = 0, & \text{if } k > 2, \quad \forall k = 2,..N \end{cases} \tag{4.76}$$

$$MSE_k = \begin{cases} \begin{cases} \Re(Factor_k)^2, & \text{if } \Im(I_{k+1})^2 = 0 \\ \Im(Factor_k)^2, & \text{if } \Re(I_{k+1})^2 = 0 \quad k <= 2 \\ (\frac{\Re(Factor_k)}{\Im(I_{k+1})} + \frac{\Im(Factor_k)}{\Re(I_{k+1})})^2, & Otherwise \end{cases} \\ \begin{cases} \begin{cases} X_{itr} = -(\Im(Factor_{k-2})\mathrm{j}/\Re(I_{k-1})), & \text{if } \Im(I_{k-1})^2 = 0 \\ X_{itr} = (\Re(Factor_{k-2})\mathrm{j}/\Im(I_{k-1})), & \text{if } \Re(I_{k-1})^2 = 0 \\ X_{itr} = (\Re(Factor_{k-2})\mathrm{j}/\Im(I_{k-1})), & Otherwise \end{cases} \\ \begin{cases} (\Re(Factor_k + X_{itr}I_{k-1}))^2, & \text{if } \Im(I_{k+1})^2 = 0 \\ (\Im(Factor_k + X_{itr}I_{k-1}))^2, & \text{if } \Re(I_{k+1})^2 = 0 \\ (\frac{\Re(Factor_k + X_{itr}I_{k-1})}{\Im(I_{k+1})} + \frac{\Im(Factor_k + X_{itr}I_{k-1})}{\Re(I_{k+1})})^2, & Otherwise \end{cases} \end{cases} \\ \forall k = 1, 2, ..(N-1) \end{cases} \quad k > 2 \tag{4.77}$$

$$MSE = \sum_{k=1}^{(N-1)} MSE_k \tag{4.78}$$

$$X_{kk} = \begin{cases} 0, & \text{if } k = 1 \\ \begin{cases} -(\Im(Factor_{k-1})\mathrm{j}/\Re(I_k)), & \text{if } \Im(I_k)^2 = 0 \\ (\Re(Factor_{k-1})\mathrm{j}/\Im(I_k)), & Otherwise \end{cases}, & \text{if } k <= 3 \\ \begin{cases} \begin{cases} -\frac{\Im(Factor_{k-1} + X_{(k-2)(k-2)}I_{k-2})\mathrm{j}}{\Re(I_k)}, & \text{if } \Im(I_k)^2 = 0 \\ \frac{\Re(Factor_{k-1} + X_{(k-2)(k-2)}I_{k-2})\mathrm{j}}{\Im(I_k)}, & Otherwise \end{cases} & \text{if } k > 3 \\ \forall k = 1, 2, ..N \end{cases} \end{cases} \tag{4.79}$$

MSE 4.78 is used in Iterative Method(II), as one of the criteria to find one possible solution. Find the lengths and compensating X values using 4.79 from the generalized method. MSE must be as minimum as possible. $N-1$ Factor equation's are obtained, where these must be purely 0 for a given set of lengths and Reactance(X) of dipoles, where both were unknown. Method 4 is used for solving N dipoles given Uniform excitation coefficients which gives one of the possible solution with Initial Lengths = 0.5λ for all dipoles.

The structure designed in this project has the advantage of being simple and excited by a single source thereby reducing the complexity of the feed network drastically. Uniform endfire arrays were the prime focus of this project and these arrays can give a maximum directivity of $\frac{4L}{\lambda}$ with L being the length of the dipole. Work done in [14] explains how the Chebyshev polynomial can be modified to obtain high directivity arrays. In Section. 4.6, the derivation of the excitation coefficients required to develop such an array is explained.

4.6 Chebyshev variant polynomial for highly directive arrays

Consider the Chebyshev variant polynomial, [2],

$$T_M(\theta) = \begin{cases} cos(Mcos^{-1}x), & |x| < 1 \\ cosh(Mcosh^{-1}x), & |x| > 1 \end{cases} \tag{4.80}$$

where,

$$x = x_m cos(\frac{\Psi(\theta)}{2}) \tag{4.81}$$

$$\Psi(\theta) = kd(cos(\theta) - 1) \tag{4.82}$$

where M is one less than the number of antennas in the array and $T_M(\theta)$ denotes the array factor of the array oriented along the z-axis.

In an antenna design, as the side lobe level (SLL) reduces, the half power beam width (HPBW) increases. In the usual Chebyshev array design, an array of any SLL can be synthesised. However, work in [14] explains how control over both SLL and HPBW can be obtained. This is done by introducing a parameter called δ in equation 4.81.

$$x = x_m cos(\frac{\Psi(\theta)}{2} + \delta) \tag{4.83}$$

4.6.1 Derivation of x_m and δ

With SLL in dB and HPBW in radians as the inputs, the parameters of the Chebyshev variant polynomial are derived. The radiation pattern which is assumed to be normalized has a maximum of 0dB. With SLL specified, the absolute value of the maxima is derived. This maxima occurs for endfire when θ is 0. As $|x|$ will be greater than 1 in such a case, the value of the maxima is substituted in the first part of equation 4.80. The magnitude at HPBW and the corresponding value for the angle is substituted thus giving rise to two equations which are solved simultaneously to obtain the two desired parameters. The array factor $T_M(\theta)$ can be expressed as the sum of electric fields of isotropic antennas, equation 4.84.

$$T_M(\theta) = \Sigma_n C_n e^{j\frac{n\pi}{2}cos(\theta)} \tag{4.84}$$

In order to derive the excitation coefficients C, principles of Fourier series is used, [2].

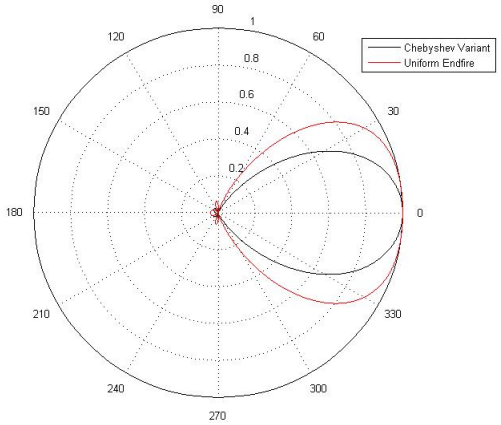

Figure 4.25: Improvement in directivity using excitation coefficients derived using [14]

Consider an example to illustrate the process explained. Let the input parameters be specified in the following manner for an array of five dipoles:

1. SLL is required to be 15dB below maxima.
2. HPBW needs to be 37^o or 0.64577^c.

If E_{max} denotes the maximum value of the electric field in the absolute scale, its value is determined by equation 4.85.

$$10log(E_{max}^2) = 15 \tag{4.85}$$

We get this value to be 5.623. This value is $\sqrt{2}$ times the value at HPBW. As explained previously, the two equations with values for half power and maxima are obtained with angles substituted appropriately.

$$cosh(4cosh^{-1}(x_m cos(\tfrac{\pi}{4}(cos(0.64577) - 1) + \delta)) = 3.976$$
$$cosh(4cosh^{-1}(x_m cos(\delta)) = 5.623$$

Upon solving them, x_m is found to be 1.2108 and δ equals -0.1972^c. Invoking equation 4.84 the excitation coefficients are derived using Fourier series method. Let cos(θ) be called ξ. The period is observed to be 4. Thus it can be rewritten as,

$$T_M(\theta) = \sum_{n=-2}^{2} C_n e^{j\frac{n\pi}{2}\xi}$$

C_n is determined by taking the inverse Fourier series.
The directivity of this superdirective endfire array is much better than that of an uniform endfire array with lower side lobes as evidenced by Fig. 4.25.

4.6.2 Synthesis of highly directive arrays with mutual coupling

In the case of endfire arrays the excitation coefficients were used to derive the input currents in the dipoles. Likewise, for highly directive arrays, the input currents are derived in a similar manner. While endfire arrays had the excitation coefficients which were either purely real or purely imaginary the methods explained in Section. 4.4 can be used without encountering impediments. However, as the C values take on forms with both real and imaginary parts, it was observed empirically that the same method took longer to converge or sometimes never converged with a suitable minimum. In order to cater to such cases, the former methods were tweaked to obtain the desired values and these methods are explained in the following section.

4.7 Methods to catalyze convergence

Different methods were explained in Section. 4.4 to arrive at the lengths and stub reactances of the dipoles. As explained, when the excitation coefficients have non-zero values for both real and complex parts, the convergence criteria which is the mean squared error(MSE) needs to be taken differently. This chapter explains the different approaches used to deal with such a situation.

4.7.1 Weighted MSE

Previously, in iterative method(II), the MSE was the square of errors. None of its constituents were given special preference. The reactances of the dipoles were obtained as,

$$X_1 = 0 \tag{4.86}$$

$$X_2 = \frac{\Re(Factor1)j}{\Im(I_2)} \tag{4.87}$$

$$X_3 = \frac{-(\Im(Factor2)j)}{\Re(I_3)} \tag{4.88}$$

$$X_4 = \frac{(\Re(Factor3 + X_2 I_2)j)}{\Im(I_4)} \tag{4.89}$$

It can clearly be observed that $Factor1$ occurs in two places-it is featured in equations involving X_2 and X_4 in the form of X_2. It would be prudent if there were lesser error in $Factor1$ and hence weights need to be introduced. This method was executed for random set of excitation coefficients and in most cases, the number of iterations required for convergence was found to be lesser for MSE with weights.

The weights were determined empirically for four dipoles. With excitation coefficients as,

$$\begin{aligned} C_1 &= 1 + j \\ C_2 &= -1 + 2j \\ C_3 &= -2 - 2j \\ C_4 &= -2 - 2j \end{aligned}$$

the case with $Factor1$ multiplied by a factor of 2.5 gave the best result in terms of convergence time. The Fig. 4.26 brings out the difference in the two methods for the same number of iterations.

This method has been used to deal with coefficients derived using the Chebyshev

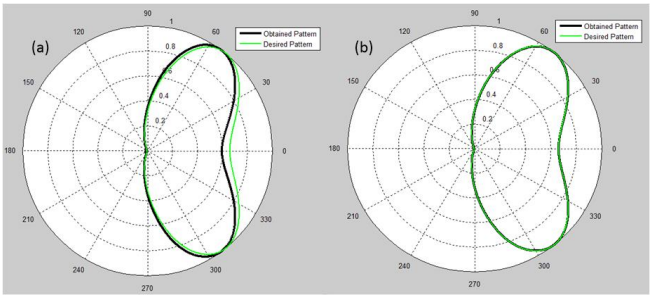

Figure 4.26: (a). Radiation pattern obtained from iterative method(II),(b). Radiation pattern obtained by considering weights for MSE

variant polynomial for cases which failed using Approach IV.

4.7.2 Using radiation pattern overlap for convergence

The main requirement of this project is to mitigate the effect of mutual coupling and the results are analyzed based on the radiation pattern. It is therefore logical to consider this parameter for convergence. In this method, the radiation pattern after every iteration is obtained and checked for divergence from the desired pattern. For the structure designed in this project, the equation for radiation pattern is given as-

$$Intensity = (E_n + E_{n-1} e^{j\frac{pi}{2}cos(\phi)} + ... + E_1 e^{j(n-1)\frac{pi}{2}cos(\phi)})^2$$

with E_n denoting the electric field of the n^{th} element.

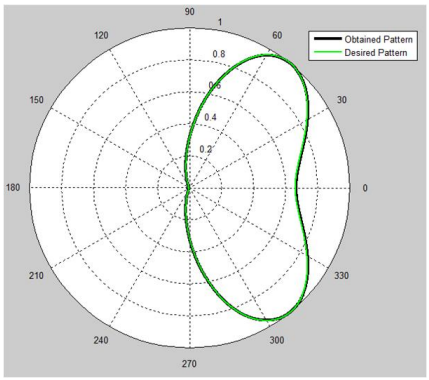

Figure 4.27: Radiation pattern obtained by considering radiation pattern match

For every value of ϕ starting from 0 with an interval of 0.001^c to π^c, the value of intensity is computed and stored in a matrix. A similar matrix is obtained for the ideal case. The matrices are subtracted and individual elements squared to derive the error matrix. The minimization of the sum total of the elements of the error matrix is considered as the convergence criteria. Lengths are iteratively varied in a manner similar to iterative method(II) until the error is reduced to a an infinitesimal quantity. This method assures desired result in most cases.

The drawback in using such a method is the time required for convergence. As the field pattern needs to be derived during every iteration, it requires a large duration of time to execute. It also has a very low tolerance for error as even with an error of 0.0885, the pattern does not overlap completely as shown in Fig. 4.27 for the same set of excitation coefficients considered for weighted MSE.

4.7.3 Prudent choice of Initial Guess

In any iteration method, the initial guess determines the flow of the algorithm. A better initial guess assures faster convergence and also outputs better values. In all the methods discussed for uniform endfire, initially half-wave dipoles were selected. The radiation pattern due to a half-wave dipole and the desired pattern is superimposed and shown in Fig. 4.28 for six and seven uniform endfire array. It was observed that

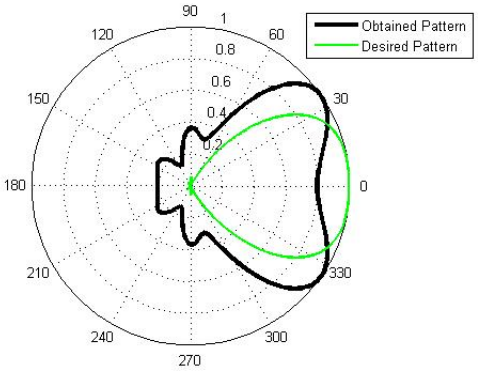

Figure 4.28: Comparison of radiation pattern with half wave dipoles and desired uniform endfire pattern for array of six dipoles

the lengths obtained for the case with mutual impedance all set to zero gave a close approximation to the desired value of radiation pattern and would therefore serve as a better intial guess as evidenced by Fig. 4.29. This fact was made use of to derive the lengths of the dipoles for the excitation coefficients derived using Chebyshev variant polynomial. To derive the initial guess, the effect of mutual coupling is completely ignored and mutual impedances are all substituted as zero. The length of the dipole farthest from the generator is set to 0.5λ. The voltage of the subsequent dipole is

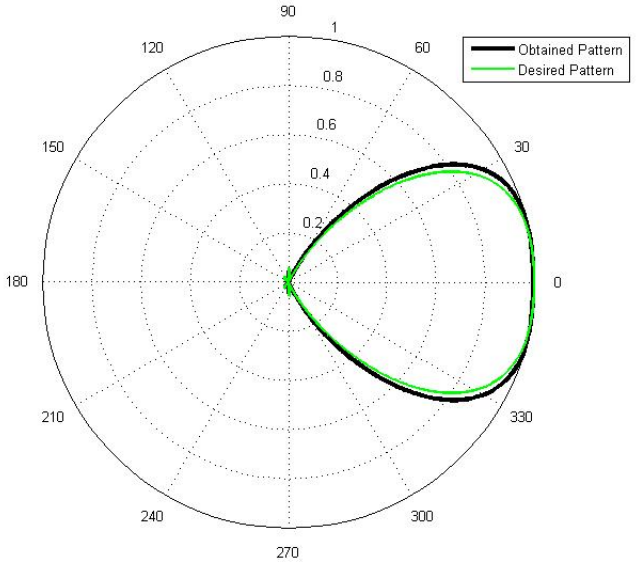

Figure 4.29: Radiation pattern comparison for the case considering zero mutual impedance

derived using the transmission line relation and it is given as,

$$V_2 = jZ_0I_1 \tag{4.90}$$

The branch equation also requires to be satisfied,

$$V_2 = Z_{22}I_2 \tag{4.91}$$

An additional parameter X_in is introduced. The relation between the impedances is given as,

$$Z_{22} = \frac{Z_r}{p^2} + X_i2 \tag{4.92}$$

which is derived using the relation between input impedance, radiation resistance and reactance. p is given by equation 4.49. The input current I_2 is given as,

$$I_2 = p\frac{C_2}{(1-cos(\frac{kl_2}{2}))}$$

These relations are combined with equations 4.90 and 4.91,

$$\frac{Z_r}{p(1-cos(\frac{kl_2}{2}))} = \Re(\frac{jZ_0I_1}{C_2})$$
$$\frac{pX_i2}{(1-cos(\frac{kl_2}{2}))} = \Im(\frac{jZ_0I_1}{C_2})j$$

The length of the dipole is varied from 0.300 to 0.900 until an appropriate value for Z_r and reactance is obtained.

4.8 Invertion of dipoles

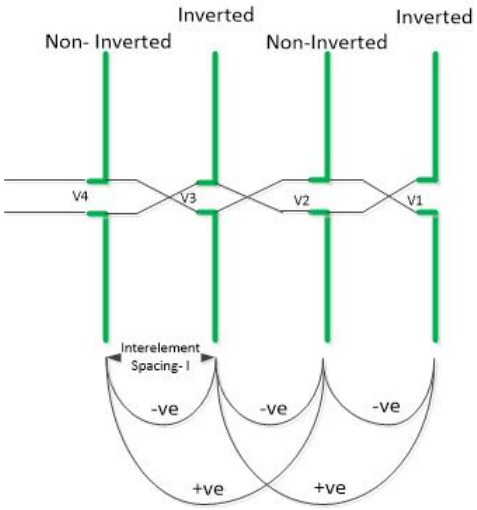

Figure 4.30: Mutual Impedance sign-convention for Inverted Dipoles

During the **initial guess** calculation process for each dipole in the structure for iterative method, sometimes situations in which radiation resistance of particular antenna turns out to be negative for all possible length values to satisfy the branch equations are encountered (without considering Mutual Coupling effect). Such situations generally arises while using highly-directive Array excitation coefficients. In such cases, concept of inverted dipole arises. The concept is simple, since negative radiation resistance of any antenna does not exist, current in that particular branch is negated and the dipole is inverted by 180^0 to eliminate the effects of negative current to tamper with the required radiation pattern.

Once initial guess for the structure is obtained, the following changes need to taken care, prior to the start of Iterative Method to calculate length values considering Mutual Coupling effects,

- The inverted dipoles while calculating initial guess in the structure must have the currents negated.
- Mutual Impedance must be negated if the dipoles are in the opposite sense. It is depicted in Fig.4.30.

Iterative method is continued as mentioned in previous sections after taking care of the above mentioned changes to obtain set of dipole length values for the structure to mitigate mutual coupling effects.

To verify the obtained set of length values, again above mentioned changes must be carried out before plotting radiation pattern for the structure by performing forward calculation with specified input voltage.

Chapter 5

Project Implementation

For the purpose of verifying the designs, codes were written on Matlab and C programming language, and execution was carried out on a 64 bit windows system. For the uniform array design, iterative method(II) was the algorithm adopted with initial lengths all fed as 0.5λ. For the synthesis of highly directive arrays, the lengths were first determined by neglecting the effect of mutual coupling and these were then used as the initial guess for iterative method(II). Simulation of the results were carried out using the HFSS tool.

5.1 Calibration Required on HFSS for the design of the structure

HFSS values are a closer estimate to practical values and this requires certain calibrations which need to be made so as to verify the results obtained theoretically which considers ideal conditions. In the design presented, the dipole antennas are connected using a two wire transmission lines. Theoretically, the dipoles and the transmission lines are analyzed discretely. However, in the practical scenario, these two structures would act as a single structure. HFSS is a tool which considers the dipoles, transmission line and stubs as a single structure and provides a full wave analysis. By comparing the results, the dissimilarities are reduced by suitable calibration and a realistic design can be arrived at.

The aim is to find the specifications (i.e. length, feed gap, thickness etc) for the design, which can be used to fabricate the structure on the PCB. The specifications need to be in the millimeter scale for our design.
The frequency of 750 MHz is used for all the HFSS analysis. The main reason is, 750 MHz corresponds to a wavelength of 400mm ($\lambda = \frac{c}{f}$), which is suitable for the scale and more practical for the analysis carried out in HFSS, in the later stages.

5.1.1 Calibration for a half wavelength dipole antenna

Since the aim is to find the specifications for the fabrication of the design, the initial analysis was carried out for the half wavelength dipole. The length of half wavelength dipole was chosen to be 0.48λ. The reason is that the thin dipole of length $(0.47 - 0.48)\lambda$ has the dipole impedance of value $(73+42.5j)\Omega$ which ideally is the impedance of a half wave dipole, from [2]. The other specifications of the dipole such as thickness and feed gap were found through various simulations. The criteria for choosing the thickness and the feed gap of the dipole are to match the radiation resistance of 73Ω

and the reactance being nearly equal to 0Ω.

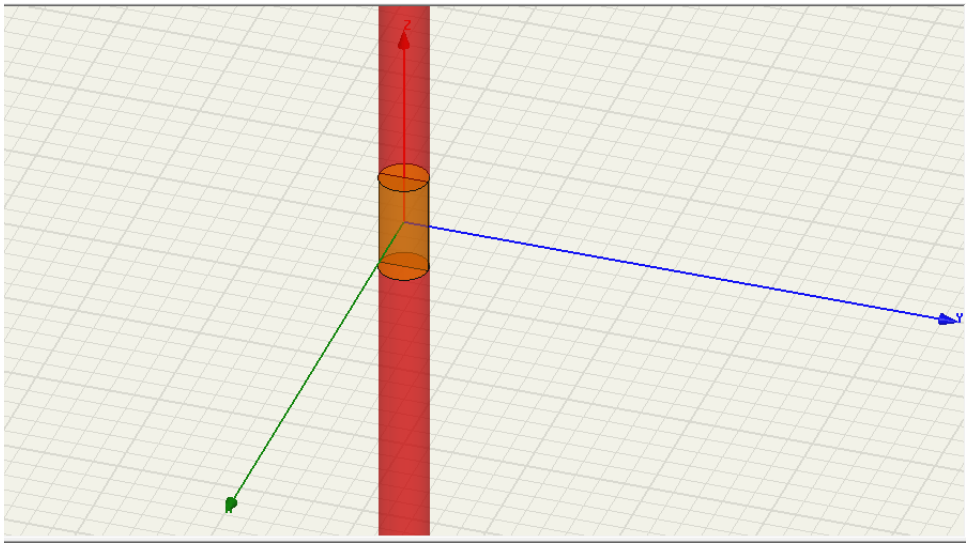

Figure 5.1: Image of the dipole

5.1.1.1 Thickness of the dipole

In theoretical calculations, the dipole is assumed to be thin having the thickness of $10^5\lambda$. But, it is hard to practically achieve this thickness and carry out the simulations. Hence several simulations were carried out in HFSS to arrive at a suitable thickness for the dipole, which can be fabricated. The thickness was varied in the range of (1-4) mm for a 0.48λ dipole and a suitable thickness was chosen.

Specifications

Frequency of operation = 750 MHz, Wavelength = 400mm
Length of the dipole = 0.48λ = 188mm
Feed gap length = 4mm

The thickness which gives the radiation resistance value of 73Ω or closer is chosen for the further analysis. From the above graph, the thickness of 1mm (radius of 0.5mm) is suitable, and henceforth in all the analysis the thickness of dipole is 1mm (radius = 0.5mm).

Table 5.1: Impedance for the various thickness of the dipole

Thickness(mm)	Resistance(Ω)	Reactance(mho)
1	74.80	9.40
2	78.63	14.72
3	84.13	15.64
4	87.86	14.45

5.1.1.2 Feed gap of the dipole

The feed gap of the dipole plays an important role in the value of impedance, because of the increase in the thickness of the dipole. The gap was varied in the range of (1-4) mm for a 0.48λ dipole and the thickness of 1mm, and a suitable feed gap length is chosen.

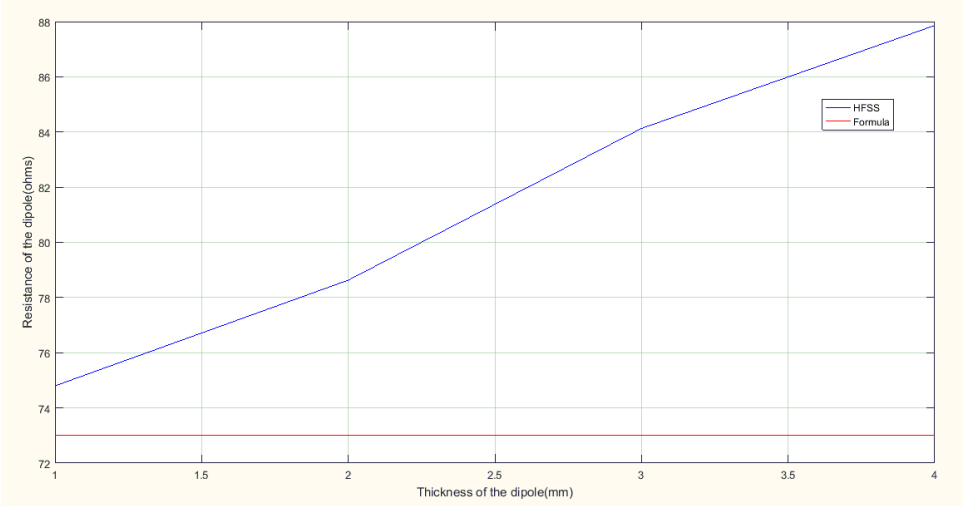

Figure 5.2: Radiation resistance v/s Thickness of the dipole

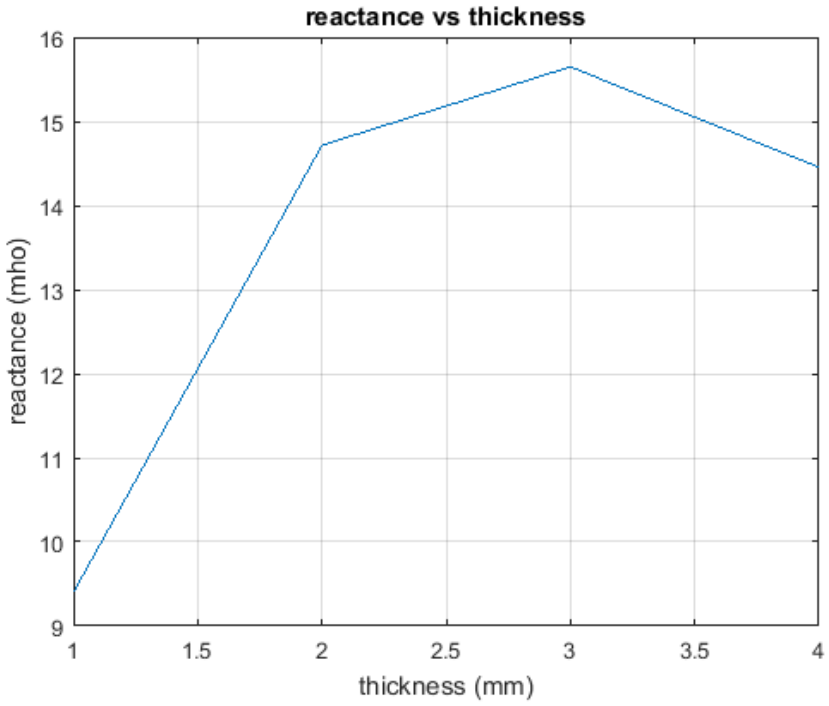

Figure 5.3: Reactance v/s Thickness of the dipole

Specifications:
Frequency of operation = 750 MHz, Wavelength = 400mm
Length of the dipole = 0.48λ = 188mm
Thickness of the dipole = 1mm
There were no significant changes in the values of the radiation resistance. The suit-

Table 5.2: Impedance for the various feed gap length of the dipole

Feed gap length(mm)	Resistance(Ω)	Reactance(mho)
1	74.40	5.15
2	74.46	7.16
3	74.36	8.04
4	74.80	9.40

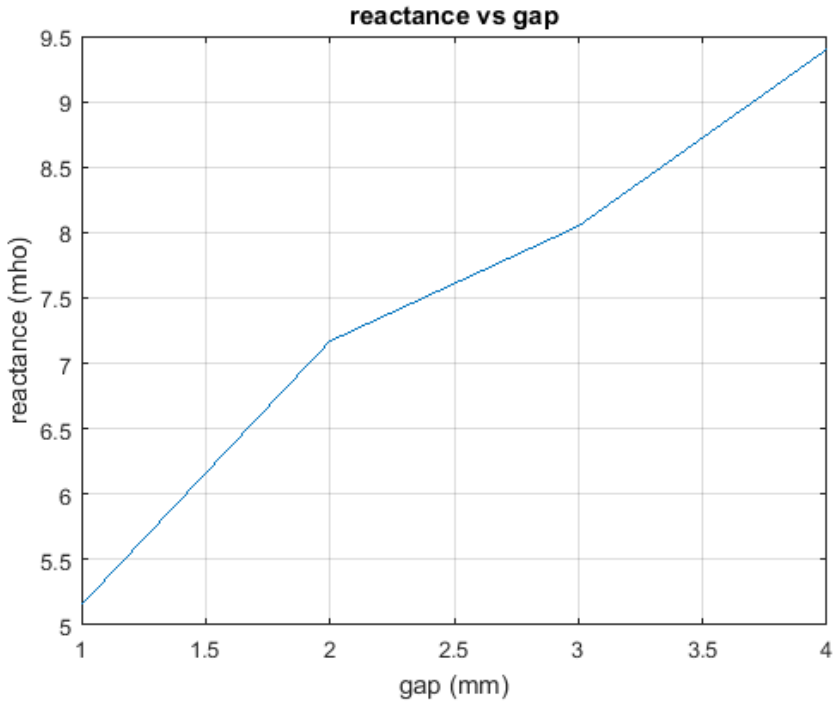

Figure 5.4: Reactance v/s feed gap length of the dipole

able feed gap length of 4mm is chosen from the graph, considering both the thickness and feed gap results. This value of feed gap is used for initial analysis, but is changed later based on the design requirements.
Therefore for the dipole of length 0.48λ, thickness 1mm, and feed gap length 4mm, the impedance is $(74.4 + 5.15j)\Omega$.

5.1.1.3 Length of the dipole

The design requires dipoles of different lengths. The simulations were carried out in HFSS to compare the radiation resistance values of the dipoles of different lengths with the theoretical radiation resistances. The thickness and the feed gap length of the dipole are taken from the previous simulation results.
Specifications:
Frequency of operation = 750 MHz, Wavelength = 400mm
Thickness of the dipole = 1mm

Feed gap length = 4mm
As the length of the dipole increases the difference in the theoretical and the practical

Table 5.3: Resistance vs length for 0.5

$Length(\lambda)$	$Impedance(\Omega)$	$RadiationResistance(\Omega)$	Reactance(mho)
0.3	21.909-220.29j	21.909	-220.29
0.35	31.216-158.93j	31.216	-158.93
0.4	44.854-91.577j	44.854	-91.577
0.45	64.471-19.819j	64.471	-19.819
0.5	92.863+55.182j	92.863	55.182
0.55	134.63+136.61j	130.72	133.27
0.6	205.75+229.16j	185.45	207.27
0.65	300.2+319.75j	238.32	253.84
0.7	469.54+406.17j	306.96	265.84
0.75	711.39+432.04j	355.5	216.02
0.8	1046.9+272.61j	361.293	94.18

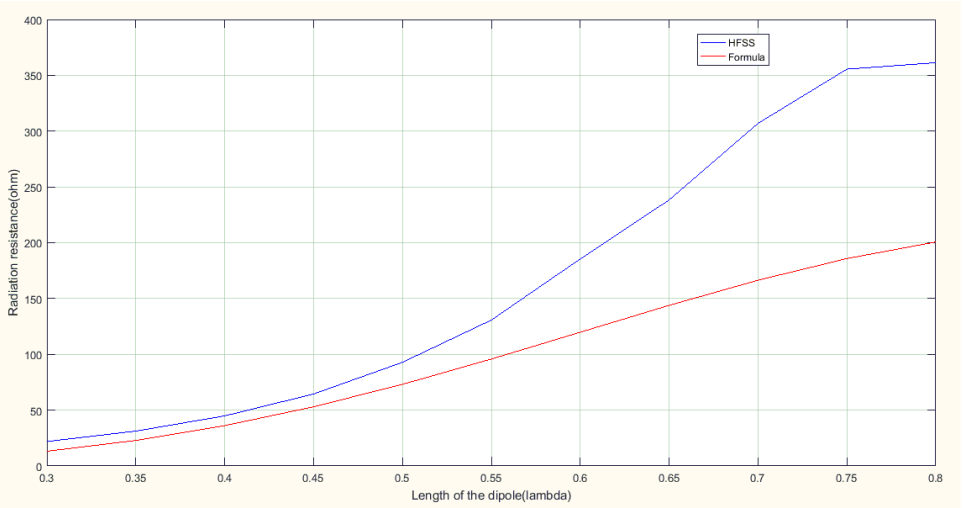

Figure 5.5: Radiation resistance v/s length of the dipole

(HFSS) values of the radiation resistance also increases. The main reason can be, as the length of the dipole increases, the effect of circular current (current in the circumference of the cross section of the dipole) is pronounced, which is mainly because of the thickness of the dipole. Another reason being, smaller feed gap length when compared to the length of the dipole.
Several other simulations were carried out for the dipole of length 0.8λ to see whether the above effects can be reduced.

- The radius of the dipole was reduced to find the radiation resistance.
  Specifications:
  Frequency of operation = 750 MHz, Wavelength = 400mm
  Length of the dipole = 0.8λ = 320mm
  Feed gap length = 4mm

Table 5.4: Resistance vs length for 0.5

Radius(mm)	*Impedance*(Ω)	*RadiationResistance*(Ω)	Reactance(mho)
1	1049.6+308.47j	362.62	106.57
0.5	1046.5+648.37j	361.55	224
0.25	981.66+899.89j	339.16	310.90
0.125	950.07+1082j	328.24	373.82
0.0625	896.32+1252j	309.67	432.56

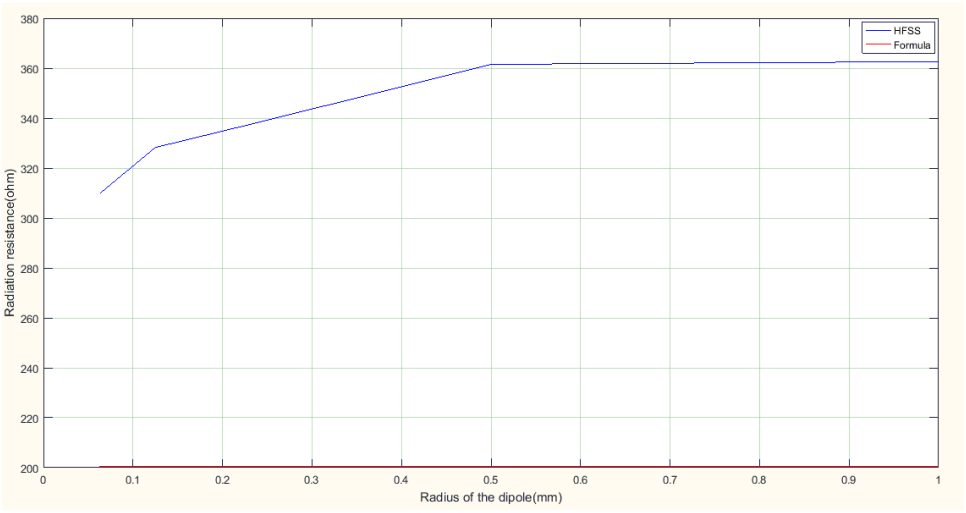

Figure 5.6: Radiation resistance v/s radius of the dipole

- For the radius of 0.0625mm, the feed gap length of the dipole was increased to see the changes in the radiation resistance.
  Specifications:
  Frequency of operation = 750 MHz, Wavelength = 400mm
  Length of the dipole = 0.8λ = 320mm
  Radius of the dipole = 0.0625mm

Table 5.5: Impedance for the various feed gap length of the 0.8λ dipole

Feed gap length(mm)	*Impedance*(Ω)	*RadiationResistance*(Ω)	Reactance(mho)
9.9	766+1230j	264.65	425
10.9	755.54+1200j	261.033	414.5
11.9	736.12+1185j	254.323	409.4
12.9	718.07+1180j	248.087	407.67
13.9	701+1176j	242.19	406.29
14.9	688.65+1168.2j	237.922	403.53
15.9	676.32+1162.3j	233.66	401.46
16.9	664.62+1156.6j	229.620	399.3
17.9	646.43+1144.1j	223.1875	395.24

From the tables 5.4 and 5.5, the difference between the theoretical and the practical values of the radiation resistance is reduced by decreasing the thickness and increasing the feed gap length.
For the radius of 0.0625mm, the frequency of operation being 750 MHz, the HFSS throws the simulation error when the structure becomes larger, i.e. when many dipoles

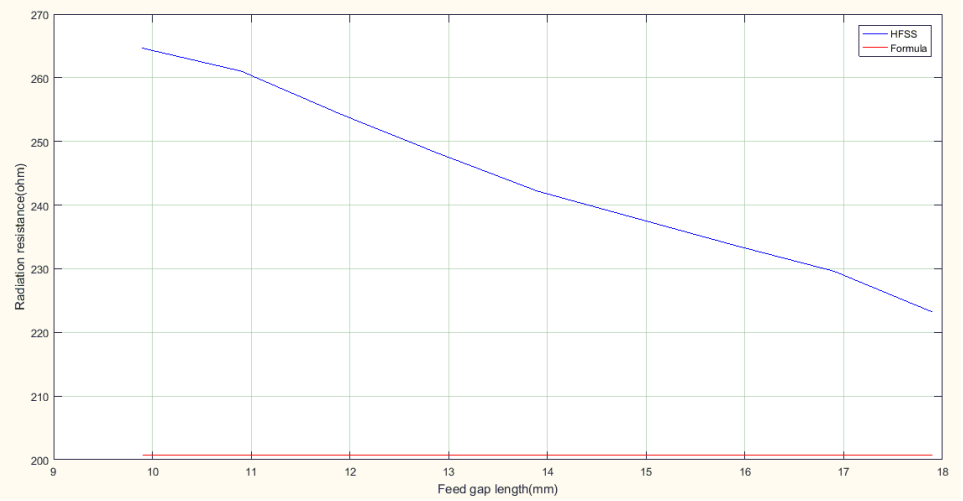

Figure 5.7: Radiation resistance v/s feed gap length of the dipole

are added to the same structure.
Hence the radius of 0.5mm is considered for the simulation and the values are calibrated wherever necessary. The length chosen for the feed gap of the dipole will be discussed in the coming chapters (feed gap length is chosen based on the design requirement).

5.1.2 Transmission Line Calibration

It was observed that the mutual impedance values between two dipoles were nearly the same and hence no calibration is carried out to match the theoretical and HFSS results. On the other hand, when transmission lines and stubs are introduced, mutual coupling arises between these elements. In order to reduce this effect, the transmission line, stubs and the dipole are placed perpendicular to each other. The characteristic

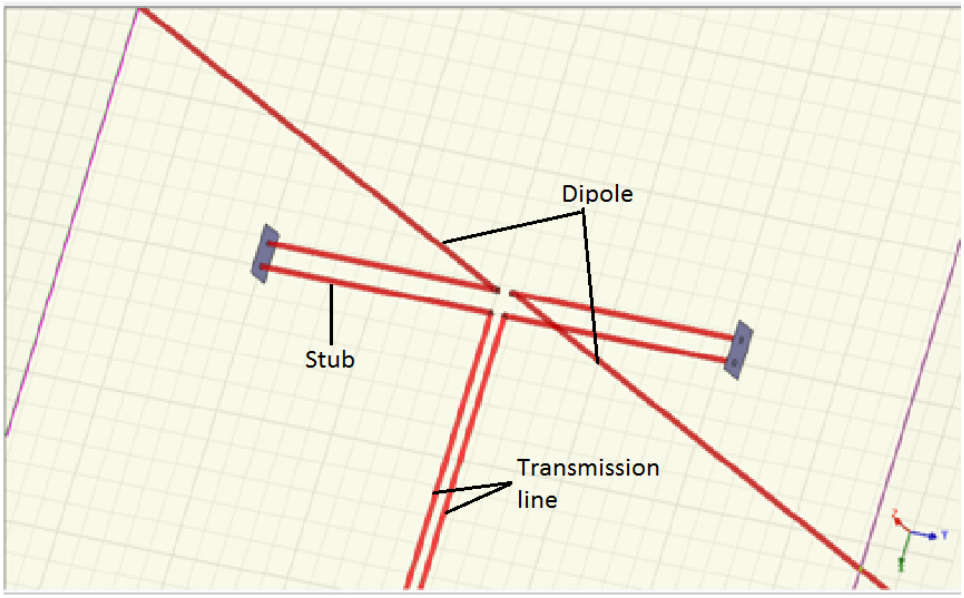

Figure 5.8: The structure of an element of the array

impedance of the transmission line is set at 200Ω.

5.1.3 Reactance Calibration

The reactance values of each of the dipoles in an array are obtained by the MATLAB code using the Iterative method(II). The reactance value (from the calculation) is achieved by placing the stubs in series with the dipole.
Since $d >> a$ gives better HFSS results (results are closer to the formula), the value of d/a is chosen to be equal to 8 for the stubs. The Z_{in} values for $d/a = 8$, and various lengths of the transmission line is obtained by simulations.
The input impedance of the transmission line of length l is,

$$Z_{in} = jZ_0 tan(\beta l) \tag{5.1}$$

where, Z_0 is the characteristic impedance of the transmission line
$\beta = 2\Pi/\lambda$, λ is the wavelength,
l is the length of the transmission line.
Specifications:
Frequency of operation = 750 MHz, Wavelength = 400mm
a=0.5mm d=4mm, $d/a = 8$
Here $Z_0 = 249.53\Omega$ (for formula)
The graph 5.9 will be used to calibrate the length of the stub for the given impedance

Table 5.6: Input impedance for the various lengths of the stub

Length of the transmission line(λ)	$Z_{in}(\Omega)$ (formula)	$Z_{in}(\Omega)$ (HFSS)
0.1	180.9j	0.047+184.32j
0.15	342.72j	0.186+363.05j
0.2	766.34j	1.1228+852.17j
0.25	Infinity	115.38-7763.4j
0.3	-766.34j	4.8059-851.59j
0.35	-342.72j	0.385-320.1j
0.4	-180.9j	0.20398-165.97j
0.45	-80.91j	0.14179-69.672j

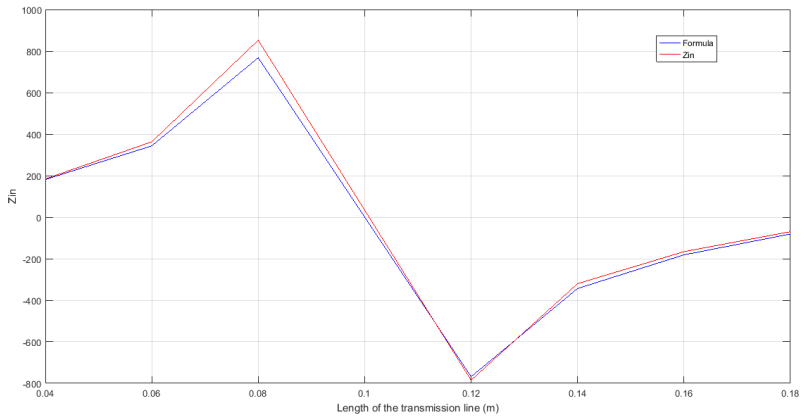

Figure 5.9: Z_{in} vs transmission line length

values.

5.1.4 Resistance calibration

The d/a for both the transmission line and the stub has been obtained. These values are used to find the feed gap length of the dipole; hence the required structure of the

design is achieved.
Therefore, the length of the gap of the dipole feed is given by = d/a of transmission line + d/a of stub – 2 * radius of the transmission line = 2.9 + 4 – 1 = 5.9mm.
The resistance and reactance values for the various lengths of the dipole, for above gap is simulated using HFSS. These values will be useful in calibration.
Specifications:
Frequency of operation = 750 MHz, Wavelength = 400mm
Thickness of the dipole = 1mm (radius = 0.5mm)
Feed gap length = 5.9mm

Table 5.7: Impedance for the various lengths of the dipole

Length of the transmission line(λ)	$Z_{in}(\Omega)$ (formula)	$Z_{in}(\Omega)$ (HFSS)	
$Length(\lambda)$	$Impedance(\Omega)$	$RadiationResistance(\Omega)$	Reactance(mho)
0.3	24.069-262.47j	24.069	-262.47
0.35	33.447-201.33j	33.447	-201.33
0.4	45.407-119.64j	45.407	-119.64
0.45	63.027-30.457j	63.027	-30.457
0.5	86.646+57.974j	86.646	57.974
0.55	121.58+153j	117.144	153
0.6	170.64+251.82j	154.345	251.82
0.65	247.1+367.29j	196.170	367.29
0.7	359.2+488.64j	235.099	488.64
0.75	558.03+621.33j	279.015	621.33
0.8	905.94+709.21j	312.994	709.21

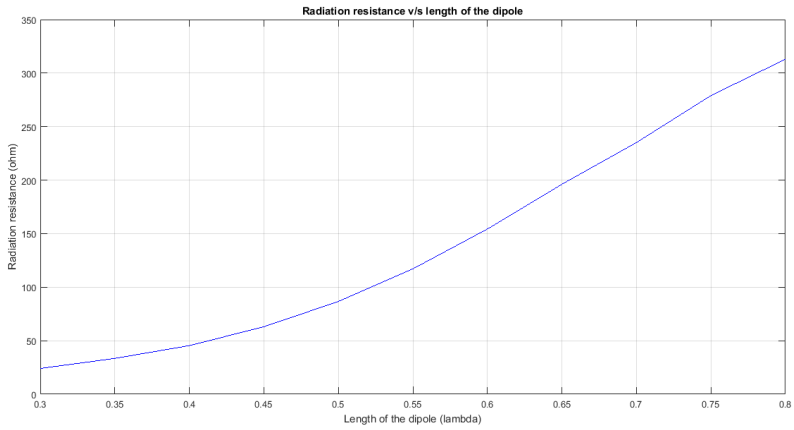

Figure 5.10: Radiation resistance vs dipole length

5.2 Calculation of length of dipole and stub

Method of calculating the length of the dipoles and stubs of the array

- The length and the reactance of each of the dipole is obtained by the Iteration method.
- The characteristic impedance of the transmission line remains fixed in all the arrays i.e. $Z_0 = 200\Omega$ and d/a = 5.8 (a = 0.5mm and d = 2.9mm) is obtained from the graph ??.

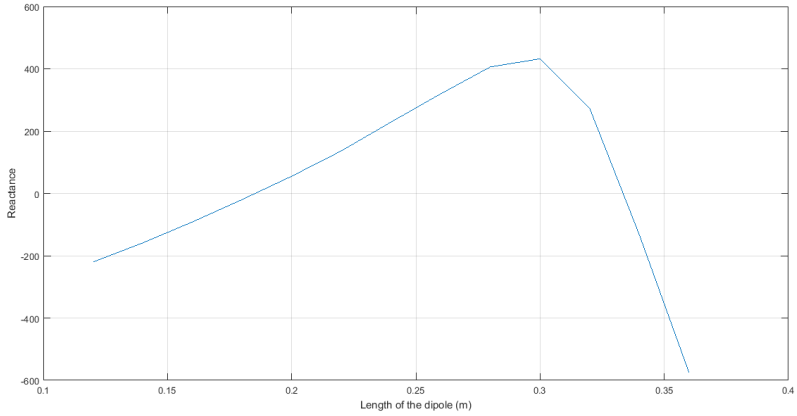

Figure 5.11: Reactance vs dipole length

- The length from the Iteration method is used to find the theoretical value of the resistance of the dipole.
- These values are mapped back to the lengths in graph **??**, which gives the length of the dipole in HFSS.
- This length is used to find the reactance of the dipole from the graph 5.11.
- Using the values of dipole reactance from the graph and the theoretical reactance from the code, the additional reactance required is obtained. This is the reactance of the stub.
  The required value of reactance = X
  The reactance of the dipole = X_R
  The reactance of the stub x = X – X_R
  The length of the stub is obtained from the graph 5.9.

Generally the stub length obtained will be greater than $\lambda/4$. This would result in additional mutual coupling between the dipoles and the stubs. Hence the required reactance of the stub is divided into half and placed on the either sides of the dipole.
General specifications:
Frequency of operation = 750 MHz, Wavelength = 400mm
Feed gap length of the dipole = 5.9mm
Thickness of all the elements = 1mm (radius = 0.5mm)
The characteristic impedance of the transmission line $Z_0 = 200\Omega$.
d/a = 5.8, a = 0.5mm, d = 2.9mm
The characteristic impedance of the stub = 249.5Ω
d/a = 8, a = 0.5mm, d = 4mm
When simulated on HFSS for 3 and 4 dipole arrays, the main lobe of the radiation pattern obtained using the HFSS was slightly lesser than the theoretical pattern. Also the radiation pattern obtained using the HFSS had a huge back lobe when compared with the theoretical pattern. The main reason was, mutual coupling between the dipoles and the stubs. Hence a measure was taken to reduce the mutual coupling.
Initially, as described earlier, stub was placed on either sides of the dipole to avoid the mutual coupling. But later it was found that the reactance value was negative, hence the single stub was placed only on one side of the dipole, but alternating sides in an array, as shown in the figure6.17.

Chapter 6

Results and Discussion

As part of this project, uniform endfire arrays and highly directive arrays were designed. The codes that were written were executed and tested for upto eight dipoles. In this chapter the results obtained for uniform endfire arrays of elements three through eight have been presented. Highly directive arrays were designed and a half power beam width of 26^o was obtained using seven dipoles. The conventions followed in naming the dipole is given by Fig. 6.1. The length of dipole 1 which is referred to as l'1 is given by the left-most element of the matrix and the succeeding values represent the lengths in an ascending order. All lengths are in terms of λ. The stub reactances follow a similar convention. The characteristic impedance is set at 200Ω for all the interlinking transmission lines.

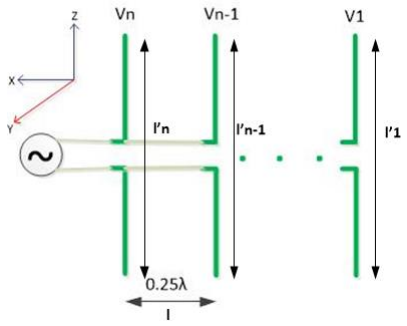

Figure 6.1: Radiation pattern comparison for the case considering zero mutual impedance

6.1 Results of Uniform endfire arrays

The following set of results were obtained for the case of uniform endfire arrays.

6.1.1 Three dipole array

The structural requirements are,

1. Length of the dipoles- [0.486,0.832,0.725]
2. Stub reactance- [0,71.40253j,41.7737j]

The radiation pattern obtained using the rectangular and absolute scale are shown in Fig. 6.2.

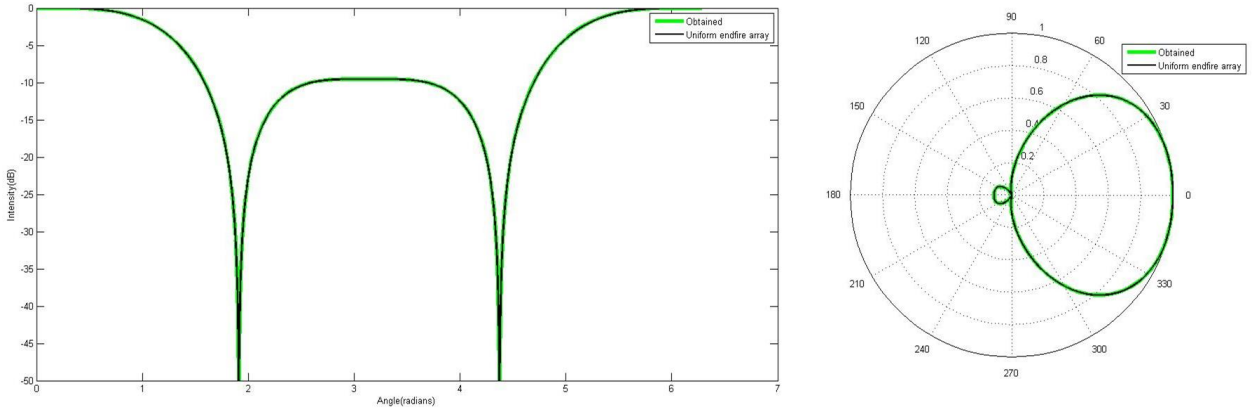

Figure 6.2: Radiation pattern for three dipole array

6.1.2 Four dipole array

The structural requirements are,

1. Length of the dipoles- [0.652,0.693,0.852,0.788]
2. Stub reactance- [0,6.240339j,217.17207j,60.130978j]

The radiation pattern obtained using the rectangular and absolute scale are shown in Fig. 6.3.

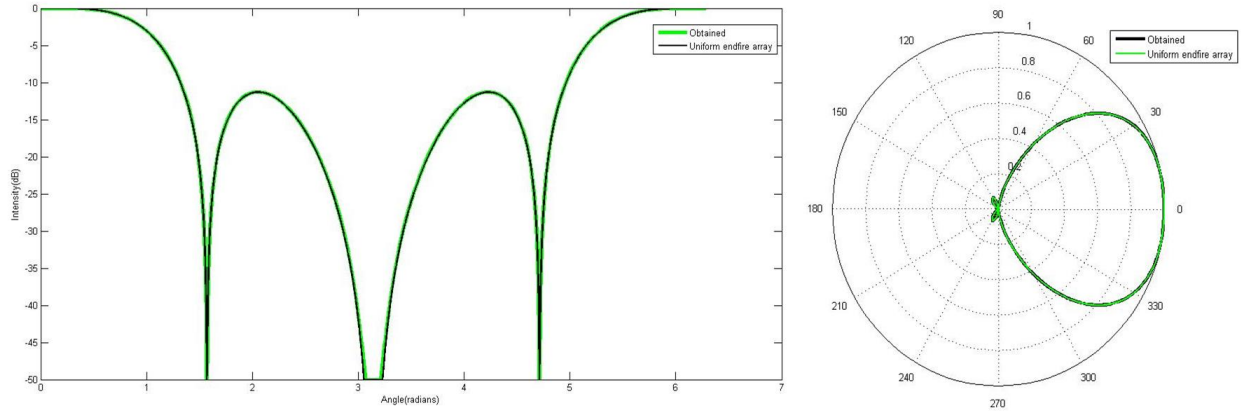

Figure 6.3: Radiation pattern for four dipole array

6.1.3 Five dipole array

The structural requirements are,

1. Length of the dipoles- [0.515,0.796,0.739,0.874,0.822]
2. Stub reactance- [0,-40.445576j,15.110921j,127.013815j,141.500206j]

The radiation pattern obtained using the rectangular and absolute scale are shown in Fig. 6.4.

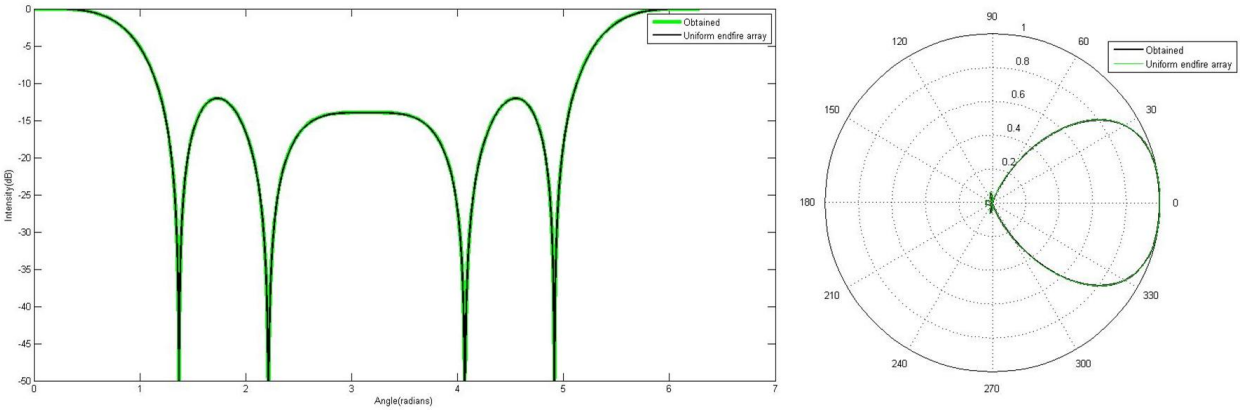

Figure 6.4: Radiation pattern for five dipole array

6.1.4 Six dipole array

The structural requirements are,

1. Length of the dipoles- [0.611,0.715,0.823,0.798,0.881,0.847]
2. Stub reactance- [0,-41.17469j,94.331275j,-30.047545j,391.633094j,58.572928j]

The radiation pattern obtained using the rectangular and absolute scale are shown in Fig. 6.5.

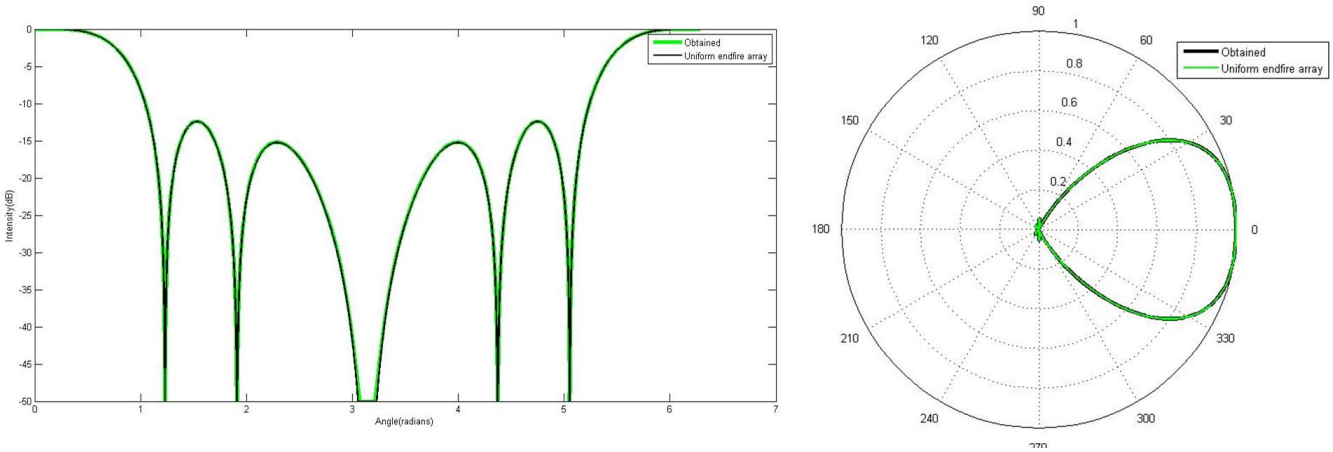

Figure 6.5: Radiation pattern for six dipole array

6.1.5 Seven dipole array

The structural requirements are,

1. Length of the dipoles- [0.532,0.775,0.753,0.856,0.825,0.890,0.866]
2. Stub reactance- [0,-87.45809j,1.746415j,-31.904706j,93.966839j,119.302951j, 287.800269j]

The radiation pattern obtained using the rectangular and absolute scale are shown in Fig. 6.6.

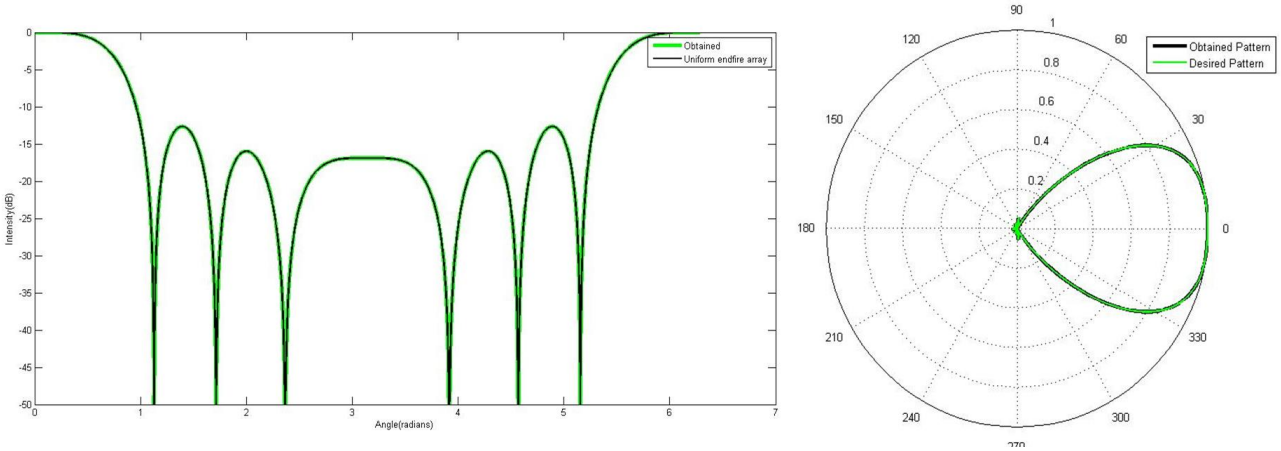

Figure 6.6: Radiation pattern for seven dipole array

6.1.6 Eight dipole array

The structural requirements are,

1. Length of the dipoles- [0.595,0.72,0.81,0.801,0.870,0.843,0.898,0.873]
2. Stub reactance- [0,-76.510772j,47.694708j,-93.340646j,251.901725j,-62.560225j, 547.197993j,49.065994j]

The radiation pattern obtained using the rectangular and absolute scale are shown in Fig. 6.7.

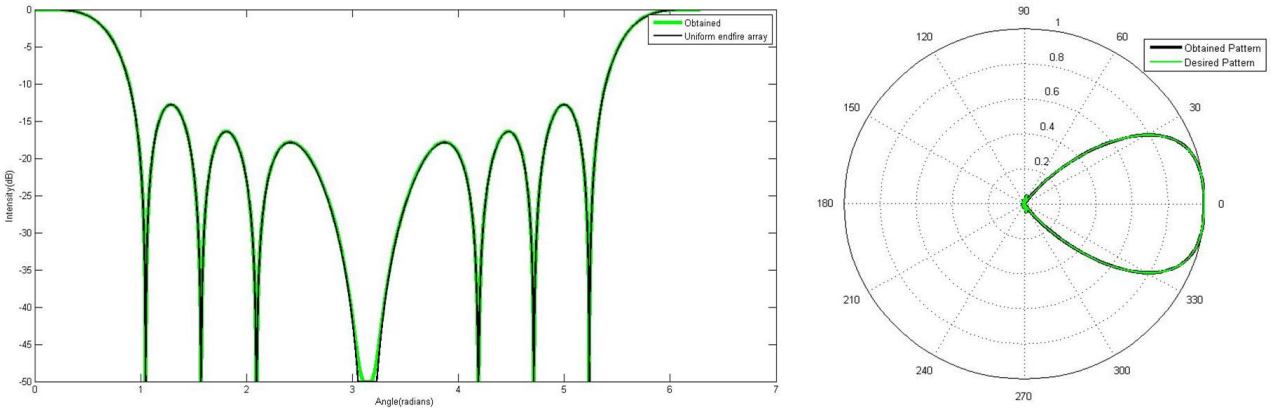

Figure 6.7: Radiation pattern for eight dipole array

6.2 Results for Highly directive endfire arrays

Highly directive endfire arrays were synthesized using the modified Chebyshev polynomials and arrays of elements ranging from four to eight dipoles were designed. This section presents the results obtained using iterative method(II) with initial lengths and reactance obtained for the case without mutual impedance coded on MATLAB and C. Here, Desired is the radiation pattern obtained directly taking the excitation

coefficients derived theoretically and Obtained is the radiation pattern obtained by calculating the currents flowing through the dipoles in the structure designed. Z_0 is fixed at 200Ω.

6.2.1 Four dipole array

The structural requirements for SLL -15dB and HPBW 40^0 are,

1. Length of the dipoles- [0.498,0.784,0.673,0.782]
2. Stub reactance- [0,-380j,-100.56j,-752.929j]
3. Excitation coefficients are- $[-1.368531666669735+0.132711274484936j, 0.954724873554108-1.784009988697605j, 0.954724873554108+1.784009988697605j, -1.368531666669735-0.132711274484936j]$
4. Dipoles required to be inverted are- nil

The radiation pattern obtained using the rectangular and absolute scale are shown in Fig. 6.8.

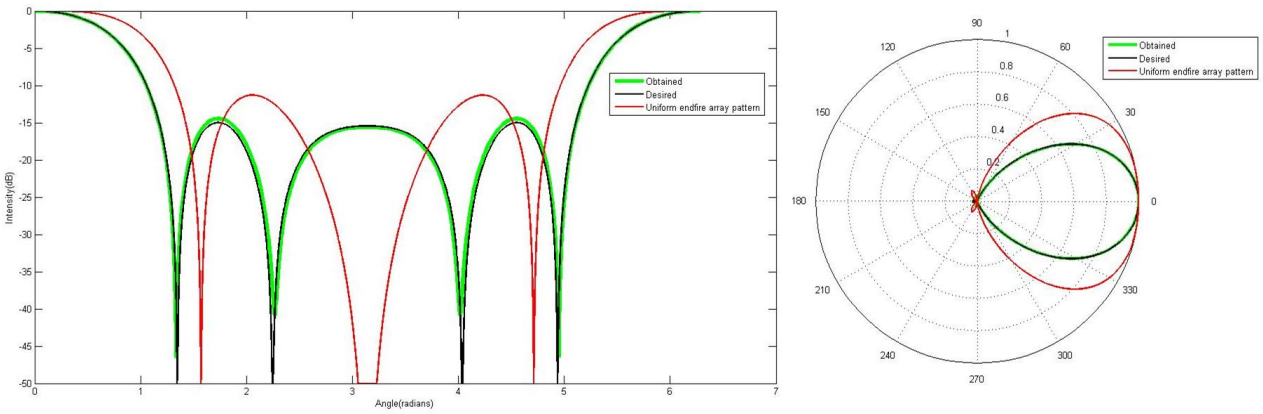

Figure 6.8: Radiation pattern for four dipole array

6.2.2 Five dipole array

The structural requirements for SLL -15dB and HPBW 37^0 are,

1. Length of the dipoles- [0.514,0.81,0.637,0.858,0.703]
2. Stub reactance- [0,-1.361330825014641e+02j,- 98.852758082710840j, - 6.695982959133905e+02j, - 3.482687769803604e+02j]
3. Excitation coefficients are- $[-0.606+0.61j, -0.42-1.01j, 1.27-4.46e-19j, -0.42+1.01j, -0.606-0.61j]$
4. Dipoles required to be inverted are- nil

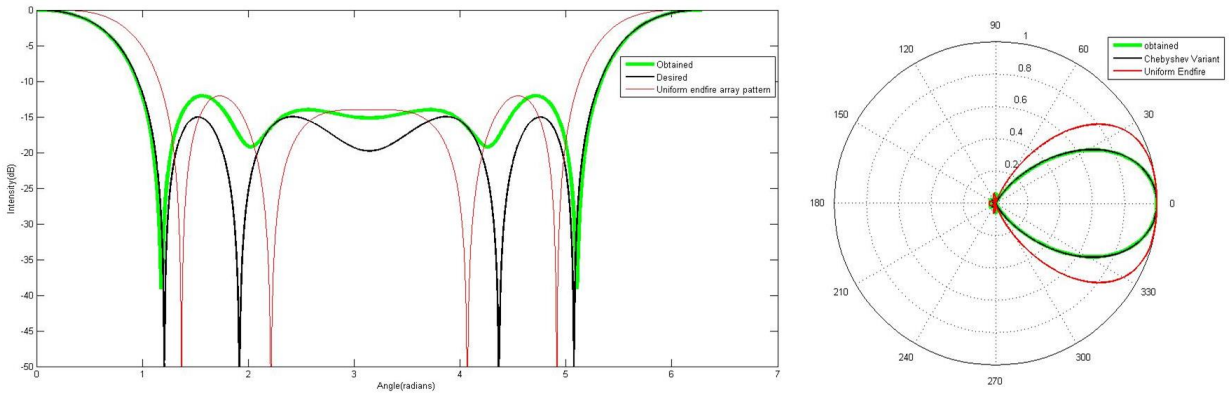

Figure 6.9: Radiation pattern for five dipole array

The radiation pattern obtained using the rectangular and absolute scale are shown in Fig. 6.9. The structural requirements for SLL -15dB and HPBW 35^0 are,

1. Length of the dipoles- [0.632,0.671,0.739,0.776,0.804]
2. Stub reactance- [0,30.933304j,22.9837j,126.343522j,400.794016j]
3. Excitation coefficients are- $[-0.524444-0.717592j, -0.52984+1.043459j, 1.362890, -0.529840-1.043459j, -0.524444+0.717592j]$
4. Dipoles required to be inverted are- dipoles 2 and 4.

The radiation pattern obtained using the rectangular and absolute scale are shown in Fig. 6.10. The structural requirements for SLL -15dB and HPBW 30^0 are,

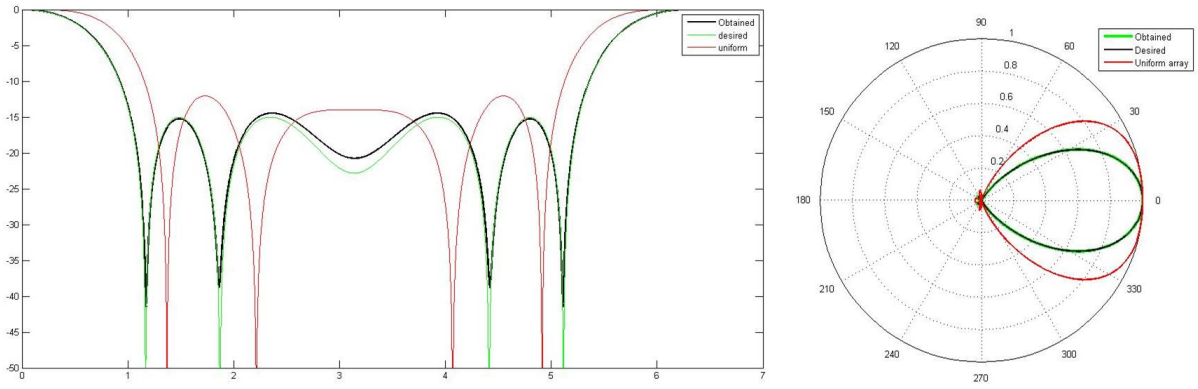

Figure 6.10: Radiation pattern for five dipole array

1. Length of the dipoles- [0.752,0.413,0.861,0.454,0.708]
2. Stub reactance- [0,8.273217j,541.624006j,45.209485j,1041.466845j]
3. Excitation coefficients are- $[-0.170927-1.007746j, -0.987913+1.169582j, 1.817625-0j, -0.987913-1.169582j, -0.170927+1.007746j]$

4. Dipoles required to be inverted are- dipoles 2 and 4.

The radiation pattern obtained using the rectangular and absolute scale are shown in Fig. 6.11.

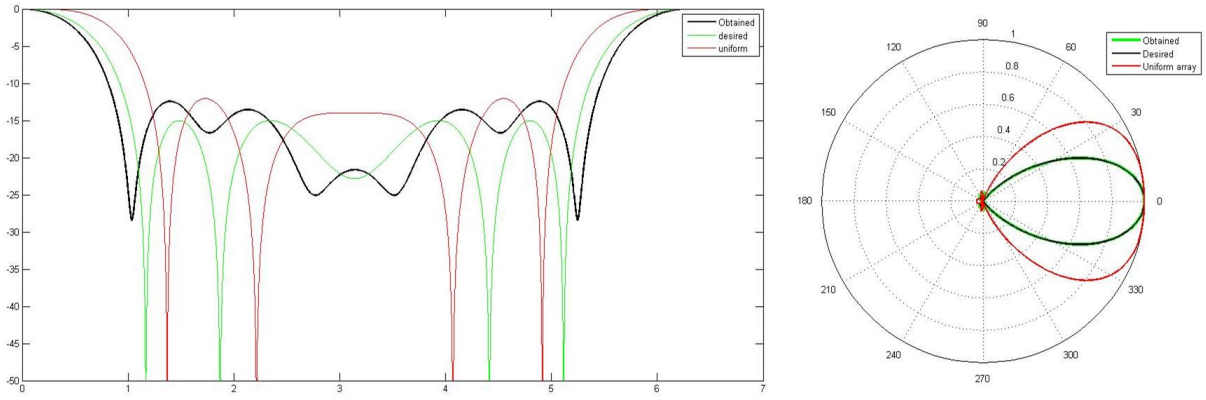

Figure 6.11: Radiation pattern for five dipole array

6.2.3 Six dipole array

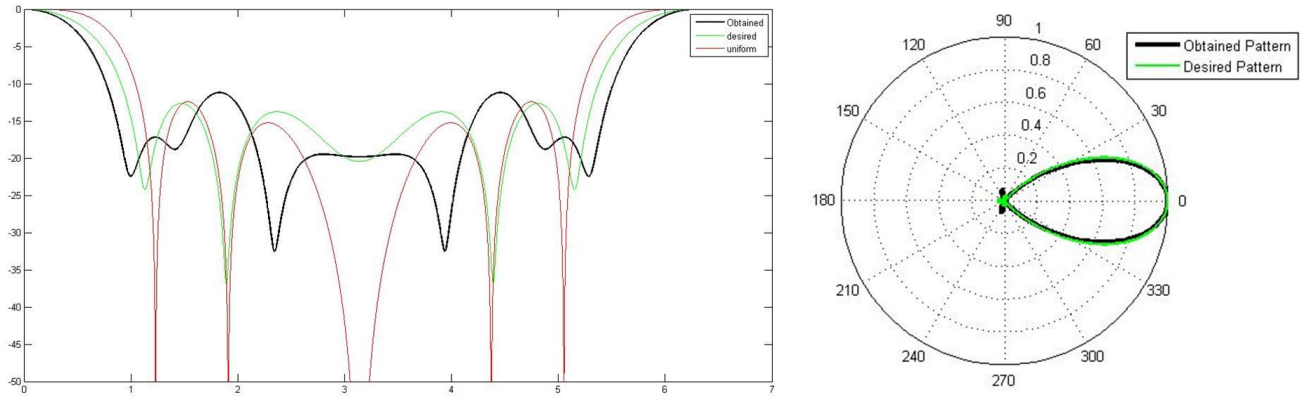

Figure 6.12: Radiation pattern for six dipole array

The structural requirements for SLL -15dB and HPBW 32^0 are,

1. Length of the dipoles- [0.567,0.757,0.603,0.796,0.802,0.591]
2. Stub reactance- [0,101.42321i,126.717951i,223.146554i, 265.49105i,374.344997i]
3. Excitation coefficients are- $[0.401544-1.116105i, -1.319119+0.19974i, 0.827508+1.346770i, 0.827508-1.346770i, -1.319116-0.199740i, 0.401544+1.116105i]$
4. Dipoles required to be inverted are- dipoles 2,4 and 6.

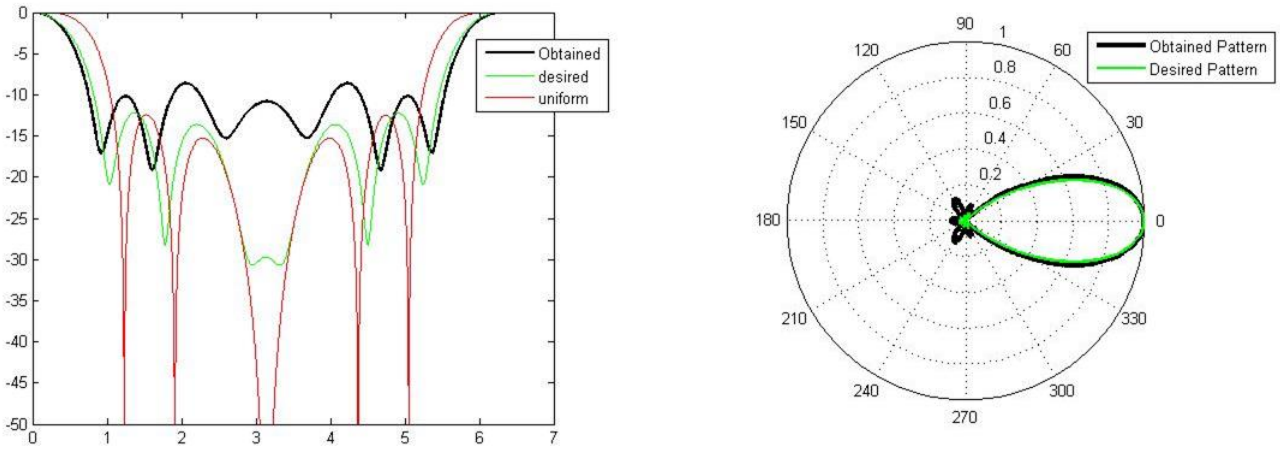

Figure 6.13: Radiation pattern for six dipole array

The radiation pattern obtained using the rectangular and absolute scale are shown in Fig. 6.12. The structural requirements for SLL -15dB and HPBW 24^0 are,

1. Length of the dipoles- [0.888,0.446,0.826,0.306,0.837,0.824]
2. Stub reactance- [0,119.746i,72.2341i,20.321134i,1896.989882i,-401.806528i]
3. Excitation coefficients are- $[1.56858-0.611972i, -2.428252-1.007806i, 1.271717+3.044289i, 1.271717-3.044289i, -2.428252+1.007806i, 1.546858+0.611972i]$
4. Dipoles required to be inverted are- dipoles 2,4 and 6.

The radiation pattern obtained using the rectangular and absolute scale are shown in Fig. 6.13.

6.2.4 Seven dipole array

The structural requirements for SLL -15dB and HPBW 27^0 are,

1. Length of the dipoles- [0.75,0.402,0.893,0.442,0.9,0.413,0.662]
2. Stub reactance- [0,18.150757i,430.333336i,-32637809310700904i, 1961.41548i,-64443322246813808i,1196.830764i]
3. Excitation coefficients are- $[0.999945-0.086083i, -0.695396-0.93768i, -0.661174+1.219961i, 1.539921, -0.661174-1.219961i, -0.695396+0.93768i, 0.999945+0.086083i]$
4. Dipoles required to be inverted are- dipoles 2,4 and 6.

The radiation pattern obtained using the rectangular and absolute scale are shown in Fig. 6.14.

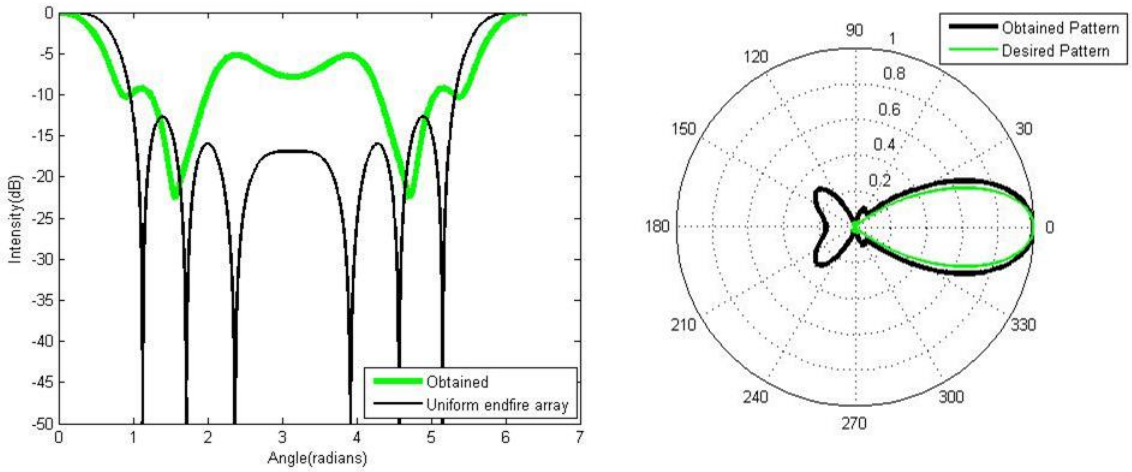

Figure 6.14: Radiation pattern for seven dipole array

6.2.5 Eight dipole array

The structural requirements for SLL -14dB and HPBW 27^0 are,

1. Length of the dipoles- [0.554,0.839,0.673,0.838,0.698,0.858,0.784,0.792]
2. Stub reactance- [0,67.916626i,-8.315167i,223.536557i,16.024683i, 563.365439i,-367.50969i,724.666726i]
3. Excitation coefficients are- $[0.761861+0.096159i, -0.083296-0.614544i, -0.704491+0.293703i, 0.513737+0.668457i, 0.513737-0.668457i, -0.704491-0.293703i, -0.083296+0.614544i, 0.761861 - 0.096159i]$
4. Dipoles required to be inverted are- dipoles 2,4, 6 and 8.

The radiation pattern obtained using the rectangular and absolute scale are shown in Fig. 6.15.

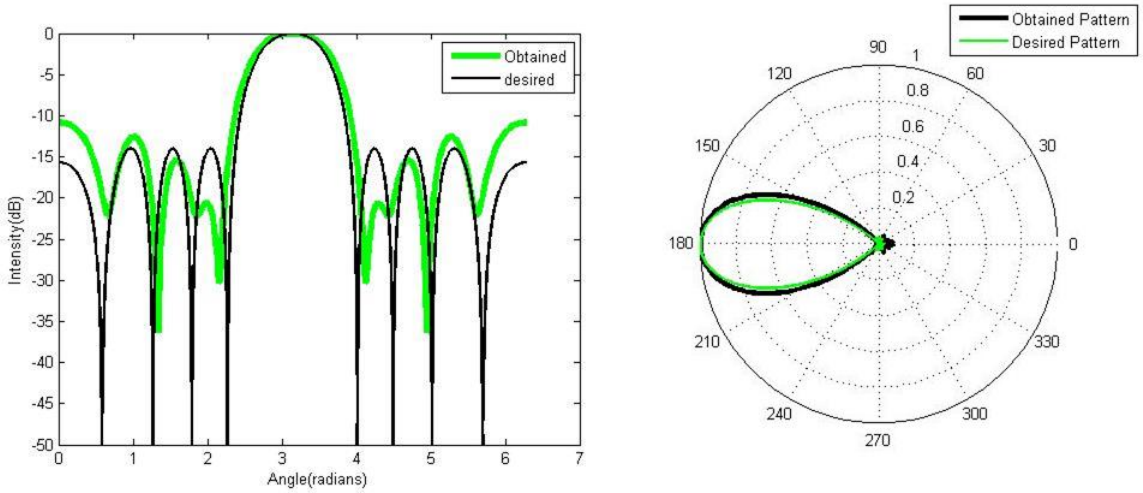

Figure 6.15: Radiation pattern for eight dipole array

The structural requirements for SLL -15dB and HPBW 25^0 are,

1. Length of the dipoles- [6.1,8.08,6.61,8.13,6.67,8.49,6.94,8.69,8.69
2. Stub reactance- [0,66.250923i,31.706433i,196.732086i,76.564976i, 784.022219i,567.128554i,-101.929058i]
3. Excitation coefficients are- $[0.761078+0.342747i, 0.061886-0.793401i, -0.976592+0.267604i, 0.653190+0.929120i, 0.65319-0.929120i, -0.976592-0.267604i, 0.061886+0.793401i, 0.761078 - 0.342747i]$
4. Dipoles required to be inverted are- dipoles 2,4, 6 and 8.

The radiation pattern obtained using the rectangular and absolute scale are shown in Fig. 6.16.

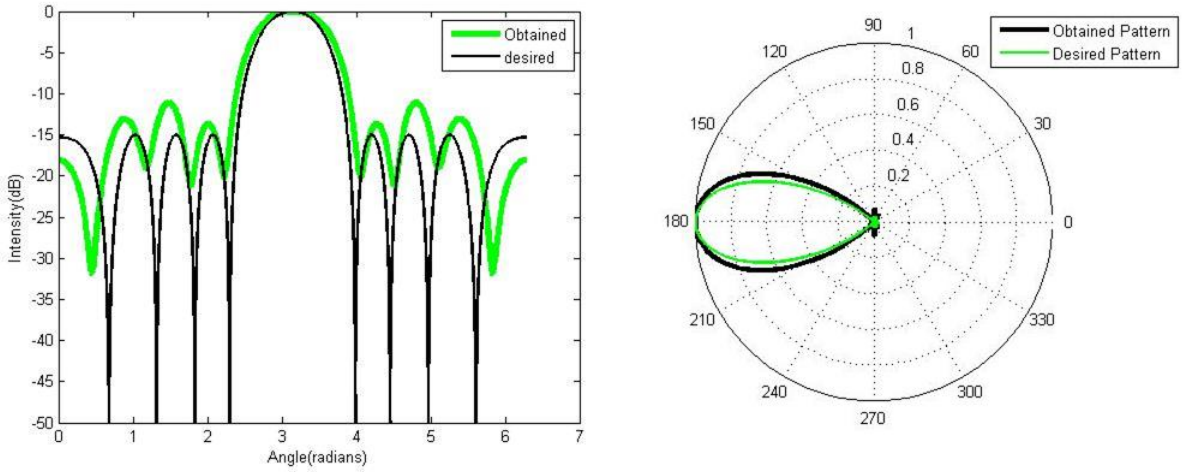

Figure 6.16: Radiation pattern for eight dipole array

Table 6.1 consolidates the results and compares the improvement for each case with the values of uniform dipole.

Table 6.1: Comparison of HPBW obtained for uniform endfire and highly directive endfire array

Elements in array	HBPW of uniform endfire(in ^{0})	Best HPBW obtained(in ^{0})	Percentage reduction (%)
4	57	40	34
5	50	30	40
6	45	32	28.88
7	42	-	-
8	39	25	35.897

6.3 HFSS simulation results

This section presents the results obtained using the HFSS simulations.

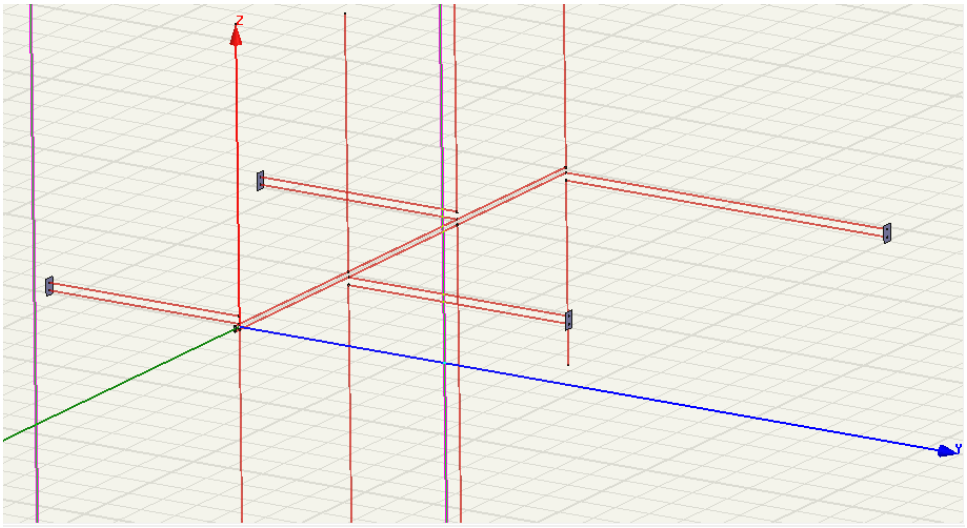

Figure 6.17: Image of the 4 dipole array

Table 6.2: Array of 4 dipoles

$Lengthofthedipole(\lambda)$	$Resistance(\Omega)$	Reactance(mho)
0.786	190	60.13
0.852	210	217.17
0.693	160	6.240
0.652	140	0

6.3.1 Uniform endfire array Results

The results from the MATLAB code for 4 dipole uniform array

By using the graphs 5.9, 5.10 and 5.11 for calibration, the new values of the length of the dipole and the stubs are obtained.

Table 6.3: Array of 4 dipoles

$Newlengthofthedipole(\lambda)$	$Reactanceofthestub(\Omega)$	Length of the stub(mm)
0.645	-289.87	144.6
0.675	-207.83	155.2
0.605	-248.76	149.5
0.585	-210	154.8

Upon this change, the main lobe of the radiation pattern was improved, but the back lobe was still present.
Similarly, the simulation was carried out for 5 dioles uniform array.

6.3.2 Super directive array Results

For the Super directive array, the method mentioned in the previous section was used to find the length of dipole and the stub, from the MATLAB simulation outputs.

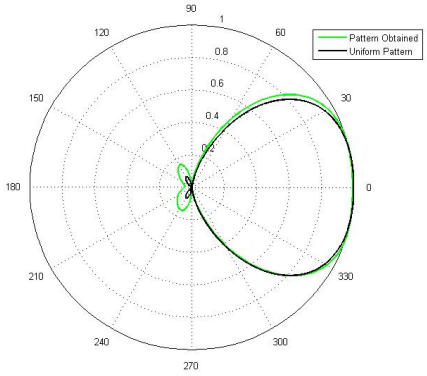

Figure 6.18: 4 dipole uniform array radiation pattern

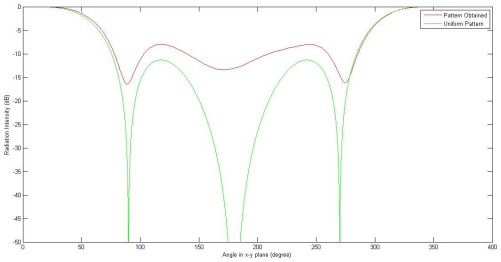

Figure 6.19: 4 dipole uniform array rectangular plot

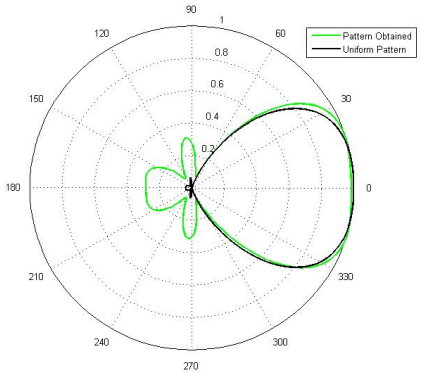

Figure 6.20: 5 dipole uniform array radiation pattern

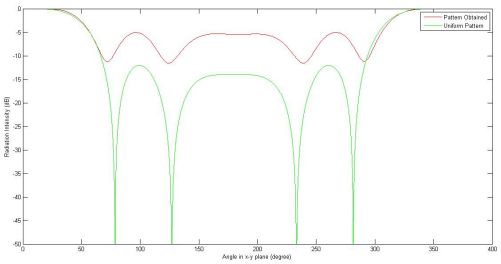

Figure 6.21: 5 dipole uniform array rectangular plot

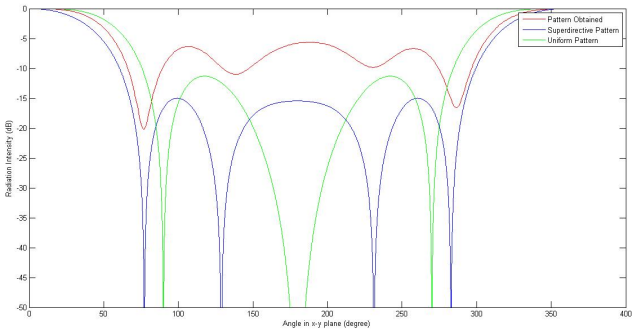

Figure 6.22: 4 dipole uniform array radiation pattern

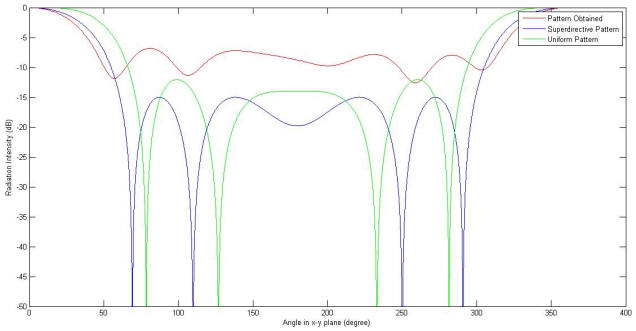

Figure 6.23: 5 dipole uniform array radiation pattern

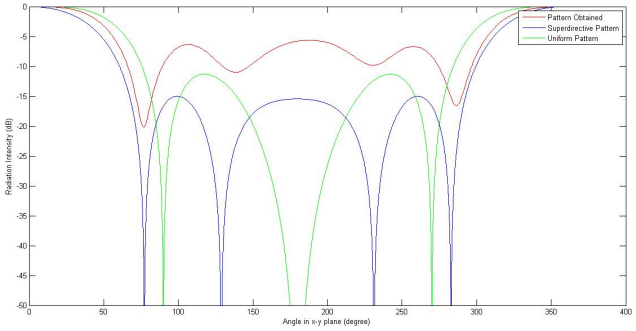

Figure 6.24: 4 dipole superdirective rectangular plot

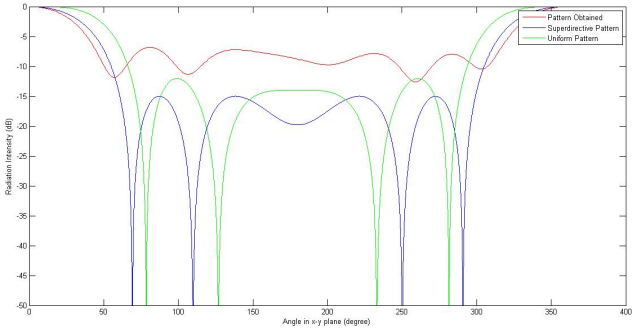

Figure 6.25: 5 dipole superdirective rectangular plot

Chapter 7

Conclusions

In this project, a simplified structure for endfire arrays was designed considering mutual coupling. All the dipoles were connected parallelly to the same pair of transmission lines thereby greatly simplifying the feed network compared to other array feeds. Uniform endfire arrays were designed and verified using codes written on Matlab and C programming language upto eight elements. Highly directive arrays were synthesized and a half power beam width improvement(HPBW) of 40% over uniform endfire for five dipoles was observed. The results have been tabulated in Table 6.1. HFSS simulations were carried out which further solidified the results obtained. Most super directive arrays have very good directivity but very poor efficiency as it requires a very high input current of the order of a few millions to produce an output current in the order of a few amperes. Work done in this project establishes that it is possible to attain a high directivity while maintaining a high efficiency by varying the length of the dipoles and using the radiation resistance itself to set the required branch currents. By making use of the radiation resistance alone the efficiency was enhanced due to the absence of the I^2R loss.

Another inference that can drawn is that the values obtained for the lengths by neglecting the effects of mutual coupling serves as a feasible starting point for an iterative solution method. It was also seen that by maintaining an inter-element spacing of 0.25λ it was possible to control the side lobe levels and have stringent control over the radiation pattern.

Control of both the SLL and HPBW simultaneously was found possible using the modified Chebyshev polynomial when the inter-element spacing was maintained at 0.25λ. The HPBW of all the arrays designed were found to be much better than that of corresponding endfire arrays. However, there was a degradation in SLL for a few arrays. In the case of five dipoles a gain of nearly 4dB was observed with both reduced SLL and HPBW. This proves the existence of a solution which can greatly improve the directivity of the array. Better algorithms which direct the search space in a better manner would need to be developed.

The future work entails the development of a better algorithm or adopt techniques like Newton Raphson method so as to ensure a better convergence value for the design of highly directive endfire arrays. Work in this project dealt with arrays upto eight elements and a directivity of 25^0 was observed. Arrays with more elements so as to get an even better directivity needs to be designed. Better calibrations need to be made for HFSS simulations in order to account for the losses which were not considered during the theoretical analysis-which assumed ideal conditions-so as to obtain a better match between the theoretical and HFSS results and this has been earmarked for the future.

Appendix A

A.1 Contributions to the project made by Anuktha S Nayak- 1PI13EC125

In the first phase of the project, study of the parameters affecting antenna radiation was studied and each of the parameters were derived and a detailed mathematical analysis was carried out. In order to observe its characteristics, matlab codes were written separately by the team members and results were compared. The mutual coupling effect was derived using induced emf method and coded on matlab following which the results were compared. Further, this member carried out a detailed analysis of the transmission line equations.

The next step of the project involved the development of the structure of the array and its analysis. This member carried out a detailed analysis of the structure for arrays with two, three and four dipoles. In order to mitigate the effects of mutual coupling, several methods were explored of which methods involving varying Z_0 both complex and real was devised by this member. This method paved way for the development of iterative method (II). All the methods devised were again coded separately and results were compared to ensure correctness of the end answer. This team member arrived at a generalization for N dipoles and wrote the complete C code to determine the lengths and reactances required to fully mitigate the effect of mutual coupling for uniform endfire arrays and further, carried out the derivation of the excitation coefficients required for the development of highly directive endfire arrays using modified Chebyshev polynomial for N dipoles. Codes for the same were written on matlab.

In the final stage of the project a different approach for the design of highly directive arrays was required. This member came up with the idea of adding weights to the MSE to improve the speed of the process. For the methods developed, codes were written separately on matlab and C programming language. This aided greatly in detecting faults and loopholes in the method and allowed us to reach the result faster. This member suggested the inverting of dipoles which proved essential in the case of highly directive arrays to obtain better directivity. Numerous results were presented and execution of results for three, five and seven dipole array were carried out by this member using C and matlab.

Appendix B

B.1 Contributions to the project made by Varsha V- 1PI13EC115

A thorough study of the parameters required for the analysis of arrays was carried out in the first phase of the project. As part of this process, a detailed mathematical analysis was carried out. Matlab codes were written separately by the team members and the plots obtained were compared. Mutual coupling effect was derived using induced emf method which was coded on matlab following which the results were discussed. Adding to this, this member carried out a thorough survey of the different methods in which the mutual coupling can be factored in a network analysis along with the equivalent circuit.

During the development of the structure of the array and its analysis, this member came with a generalization to deal with any number of dipoles interconnected with the transmission lines. During the algorithm development stage, the different possibilities were discussed. This member came up with the idea of making use of the iterative method keeping a constant Z_0 which greatly simplified the design. Additionally different methods used in the formative stage which lead to the development of iterative method (II) was devised by this member. All the methods were coded separately following which a comparison of the results were carried out. This team member came up with a generalization to obtain the excitation coefficients of highly directive arrays synthesized using modified Chebyshev polynomial for N dipoles.

While dealing with highly directive arrays, there are constraints on the SLL and HPBW making it hard to obtain the lengths and the reactances to mitigate mutual coupling as obtained for the case of uniform endfire arrays. This member came up with the idea of using the radiation pattern itself as the criteria for convergence. Further, as the method used is iterative, a better initial guess leads to faster and better results. This member devised a method to determine a better initial guess so as to catalyze convergence of the methods. This member came up with the generalized code for finding the lengths and reactance for N dipoles for the design of highly directive arrays. Finally, many results were presented and execution of results for four, six and eight dipole array were carried out by this member using matlab and C.

Appendix C

C.1 Contributions to the project made by Ramyashree V Bhat- 1PI13EC076

During the first phase of the project, different existing methods used to mitigate the mutual coupling efffects was studied by refering to various papers. The HFSS tool was used for the simulations. This member learnt the HFSS tool. Initially various simulations were carried out by this member to find the suitable thickness of the dipole, in practical scenario. Various simulations were carried out by this memeber to find the suitable feed gap length of the dipole.

For the dipoles of length 0.8λ and above the radiation resistance of the dipole deviated from the theoretical values. Hence various simulations were carried out by this member, to obtain the suitable radiation resistance, by varying the thickness and the feed gap length of the dipole (which is also suitable for practical scenario). The calibration was required for the theoretical values in order to simulate the structure in HFSS. This memeber, carried out various simulations and obtained the calibration graph for the characteristic impedance of the transmission line. In order to find the stub length, various simulations were carried out by this member and the input impedance calibration graph for the various lengths of the stub was obtained by this member. Since many dipoles in the structure were of length 0.8λ and above, resistance calibration graph was obtained by this member, which was used in the further simulations.

Initially, the structure had two stubs on the either sides of the dipole, to compensate the required reactance. This resulted in mutual coupling. This member gave the idea of placing the stubs on one side and in alternate positions of the dipole, which reduced the mutual coupling and gave the better results. This member carried out HFSS simulation for three, four and five dipole uniform array. The radiation pattern and the rectangular plot were obtained for comparision. HFSS simulation for four and five dipole super directive array was carried out by this member. The rectangular plot was obtained. This was used for the comparision with the MATLAB and C programming outputs. The simulation, carried out by this member, helped to analyse the structure in realistic manner, because it considered the dipoles and transmission line as a single structure.

Bibliography

[1] S. M. Amjadi and K. Sarabandi, "Mutual coupling mitigation in broadband multiple-antenna communication systems using feedforward technique," *IEEE Transactions on Antennas and Propagation*, vol. 64, no. 5, pp. 1642–1652, 2016. 2

[2] C. A. Balanis, *Antenna theory: analysis and design*. John Wiley & Sons, 2016. 2, 4.1.3, 4.6, 4.6.1, 5.1.1

[3] G. J. Burke, A. Poggio, J. Logan, and J. Rockway, "Numerical electromagnetic code (nec)," in *Electromagnetic Compatibility, 1979 IEEE International Symposium on*. IEEE, 1979, pp. 1–3. 2

[4] M. Dawoud and A. Anderson, "Design of superdirective arrays with high radiation efficiency," *IEEE Transactions on Antennas and Propagation*, vol. 26, no. 6, pp. 819–823, Nov 1978. 2

[5] I. Gupta and A. Ksienski, "Effect of mutual coupling on the performance of adaptive arrays," *IEEE Transactions on Antennas and Propagation*, vol. 31, no. 5, pp. 785–791, 1983. 2

[6] M. Hamid and R. Hamid, "Equivalent circuit of dipole antenna of arbitrary length," *IEEE Transactions on Antennas and Propagation*, vol. 45, no. 11, pp. 1695–1696, 1997. 2

[7] A. Haskou, A. Sharaiha, and S. Collardey, "Decoupling approach of superdirective antenna arrays," in *The 11th European Conference on Antennas and Propagation*, 2017. 2

[8] ——, "Theoretical and practical limits of superdirective antenna arrays," *Comptes Rendus Physique*, vol. 18, no. 2, pp. 118–124, 2017. 2

[9] S. Henault, S. K. Podilchak, S. M. Mikki, and Y. M. Antar, "A methodology for mutual coupling estimation and compensation in antennas," *IEEE Transactions on Antennas and Propagation*, vol. 61, no. 3, pp. 1119–1131, 2013. 2

[10] J. H. Kim, S. I. Cho, H. J. Kim, J. W. Choi, J. E. Jang, and J. P. Choi, "Exploiting the mutual coupling effect on dipole antennas for rf energy harvesting," *IEEE Antennas and Wireless Propagation Letters*, vol. 15, pp. 1301–1304, 2016. 2

[11] S. Y. Liao *et al.*, *Microwave devices and circuits*. Pearson Education India, 1990. (document), 4.3.1, 4.13

[12] T. Ma, Z. Li, W. T. Joines, and J. Li, "Novel design of end-fire dipole array antennas," in *Antennas and Propagation (APSURSI), 2016 IEEE International Symposium on*. IEEE, 2016, pp. 1585–1586. 2

[13] J. Rao, X. Xu, and Q. Wang, "Mutual coupling compensation of array antenna pattern," in *Communication Software and Networks (ICCSN), 2015 IEEE International Conference on*. IEEE, 2015, pp. 143–146. 2

[14] P. R. Shigehalli and S. Adhikari, "Synthesis of highly directive endfire arrays using modified chebyshev polynomials," *Procedia Computer Science*, vol. 93, pp. 81–88, 2016. (document), 2, 4.5, 4.6, 4.25